

AD-A054 995

CINCINNATI UNIV OH DEPT OF ENGINEERING SCIENCE  
AN EVALUATION OF THE MONOTONIC RESPONSE OF RENE 95 AT 1200 F.(U)  
FEB 78 D C STOUFFER

F/G 11/6

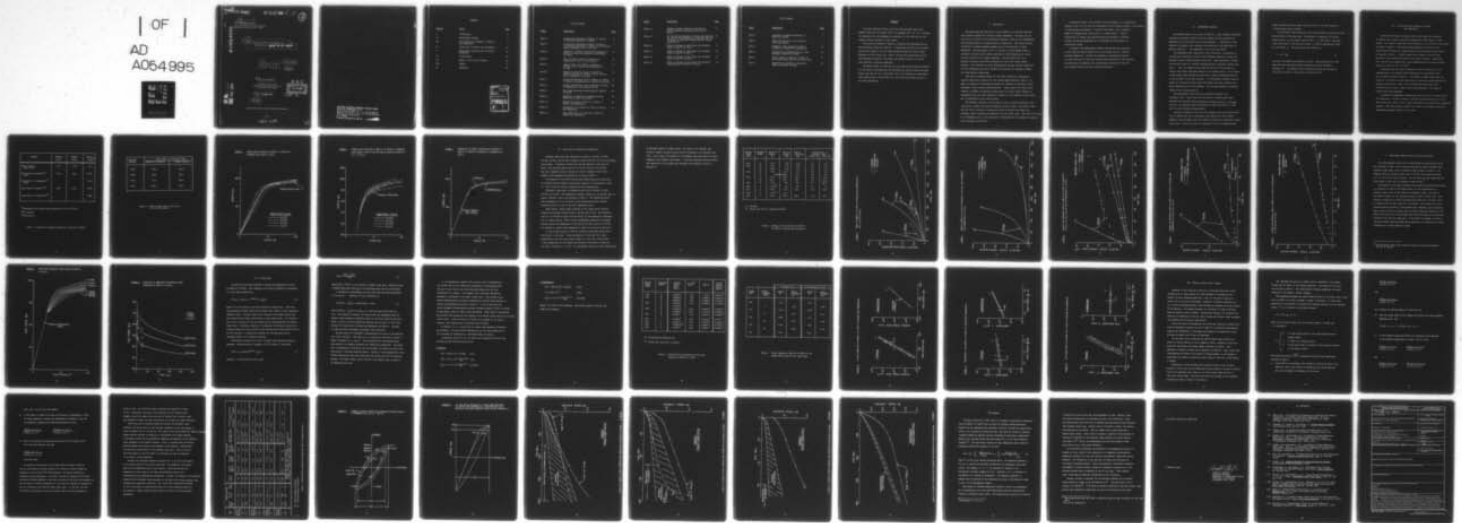
AFOSR-77-3101

UNCLASSIFIED

AFOSR-TR-78-0905

NL

| OF |  
AD  
A054995



END  
DATE  
FILMED  
7-78  
DDC

19  
AFOSR TR-78-0905  
18

FOR FURTHER TRAN 14

2  
B.S.

15  
Grant No. AFOSR-77-3101

Air Force Office Of Scientific Research  
Bolling Air Force Base, D C 20332

AD A 054995

6  
AN EVALUATION OF THE MONOTONIC  
RESPONSE OF **RENE 95 AT 1200°F.**

9  
FINAL rept.  
15 Dec 76 - 14 Dec 77

16 2307  
17 D9

10  
Donald C. Stouffer

University of Cincinnati  
Department of Engineering Science  
Cincinnati, Ohio 45221

DDC  
RECEIVED  
JUN 12 1978  
B

11  
February 1978

12 53p.

AD NO. \_\_\_\_\_  
DDC FILE COPY

Approved for public release; distribution unlimited.

1473  
410 649

4B

3000-87-0000

(S)

20020700

DDC  
RECEIVED  
MAY 15 1978

DDC LIFE COB  
20020700

**AIR FORCE OFFICE OF SCIENTIFIC RESEARCH (AFOSR)**  
**NOTICE OF TRANSMITTAL TO DDC**  
This technical report has been reviewed and is  
approved for public release IAW AFR 190-12 (7b).  
Distribution is unlimited.  
**A. D. BLOSE**  
Technical Information Officer

## CONTENTS

<u>Section</u>	<u>Title</u>	<u>Page</u>
I	Introduction	1
II	Experimental Program	3
III	The Stress-Strain Response in Tension and Compression	5
IV	Creep Tests in Tension and Compression	11
V	Relationship Between Creep and Stress Relaxation	19
VI	A Creep Model	22
VII	Effect of Prior Cyclic Fatigue	31
VIII	Summary	43
IX	References	46

ACCESSION FOR		
NTIS	Main Section	<input checked="" type="checkbox"/>
DDI	DDI Section	<input type="checkbox"/>
UNCLASSIFIED		<input type="checkbox"/>
IDENTIFICATION		
BY _____		
DISTRIBUTION/AVAILABILITY CODES		
Dist.	AVAIL.	and/or SPECIAL
A		

## LIST OF FIGURES

<u>Figure</u>	<u>Description</u>	<u>Page</u>
Figure 1	Stress-Strain Response of René 95 in Tension at Different Head Rates at 1200°F	8
Figure 2	Stress-Strain Response of René 95 in Tension at Different Head Rates at 1200°F with the Elastic Modulus Adjusted to $25.7 \times 10^6$ PSI.	9
Figure 3	Comparison of Nominal Stress-Strain Response of René 95 in Tension to Response in Compression at 1200°F.	10
Figure 4	Creep of René 95 1200°F in Tension and Compression at 184, 175 and 163 KSI.	14
Figure 5	Creep of René 95 at 1200°F in Tension at 150 KSI, and in Tension and Compression at 131 KSI.	15
Figure 6	Primary and Secondary Creep of René 95 at 1200°F in Tension at 184 KSI, 175 KSI, 163 KSI and in Compression at 184 KSI.	16
Figure 7	Primary and Secondary Creep of René 95 at 1200°F in Tension and Compression at 150 KSI and 131 KSI.	17
Figure 8	Primary and Secondary Creep of René 95 at 1200°F in Compression at 150 KSI and 175 KSI.	18
Figure 9	Short Time Isochronis Creep Curves for René 95 at 1200°F.	20
Figure 10	Comparison of Predicted and Observed Stress Relaxation of René 95 at 1200°F.	21
Figure 11	Minimum Creep Rate of René 95 at 1200°F in Tension and Compression.	28
Figure 12	Coefficient A For René 95 at 1200°F in Tension and Compression.	29
Figure 13	Time Coefficient $\beta$ for René 95 at 1200°F in Tension and Compression.	

<u>Figure</u>	<u>Description</u>	<u>Page</u>
Figure 14	Schematic Diagram Showing the Deformation History Applied to Specimens 9,11,12,13,14, and 16.	37
Figure 15	(a) The Initial Response of Virgin Creep Specimen. (b) Initial Creep Response of a Specimen That Has 40 cycles of 1.8% Total Reversed Plastic Strain (Specimen 11).	38
Figure 16	Effect of Fatigue of the Primary and Secondary Creep of René 95 at 1200°F.	39
Figure 17	Effect of Fatigue on the Primary and Secondary Creep of René 95 at 1200°F.	40
Figure 18	Effect of Fatigue on the Primary and Secondary Creep of René 95 at 1200°F.	41
Figure 19	Effect of Fatigue on the Primary and Secondary Creep Response of René 95 at 1200°F.	42

## LIST OF TABLES

<u>Table</u>	<u>Description</u>	<u>Page</u>
Table 1	Variations in Tensile properties of René 95 at 1200°F.	6
Table 2	Effect of head rate on the stress at 1.0% total strain.	7
Table 3	Summary of creep response in René 95 at 1200°F in tension and compression.	13
Table 4	Characteristic parameters for the creep response of René 95 at 1200°F.	26
Table 5	Static response of René 95 at 1200°F at the stress levels used for the creep tests.	27
Table 6	Characteristic parameters showing the effect of fatigue on creep.	36

## FOREWARD

The Final Technical Report covers all work performed under Grant AFOSR-77-3101 from 15 December 1976 to 14 December 1977. Dr. D. C. Stouffer is responsible for the management and execution of the Grant and for the research results contained in this report.

This Grant was awarded to develop a "Constitutive Representation and Life Prediction Method for Rene 95". A significant portion of the research was done off campus at the Air Force Materials Laboratory (LLN), Wright Patterson Air Force Base, Ohio 45433. The work was coordinated with the Solid Mechanics Program of the Metals and Ceramics Division of the Air Force Materials Laboratory (AFML/LLN).

The Author wishes to thank the Air Force Materials Laboratory personnel for the efforts and cooperation for providing the tensile creep and stress-strain data; Met-Cut Inc., Cincinnati, Ohio, for providing the compressive creep response data; and Mar-Test Inc., for doing the fatigue portion of the creep experiments.

## I. Introduction

The broad long term objective of this research is to develop a material life prediction method for structural engine components. One major part of the work is to develop a life prediction technique in the low (to intermediate) cycle fatigue domain of an engine alloy at temperature. This should include the ability to handle cumulative damage due to load histories in three dimensions. The second major part is to develop a finite element model to calculate the stress and/or strain histories in three dimensions at various critical locations of an engine component. The third major part is to develop an accurate constitutive equation for use in the finite element analysis. This should be in three dimensions and include variable temperature and load histories, and also be capable of accounting for cumulative damage and creep-fatigue interactions.

This work is directed toward the third major objective, developing an accurate constitutive equation for the typical engine material, René 95. To begin the analysis an experimental program was conducted to establish a broad catalogue of basic response characteristics. These include the stress-strain response in tension at different strain rates; the stress strain response in compression; and, the creep response in tension at five different stress levels and in compression at four stress levels.

The monotonic response in creep data was used to develop isochronis creep curves and to predict the stress-relaxation for short times. The René 95 creep data was used to construct a constitutive model to predict the primary and secondary creep in tension and compression at any stress level. This model will serve as a fundamental part of the constitutive relationship for the mechanical response due to variable load history.

An important factor to be included in this development of a constitutive equation, which is to be used for predicting low cycle fatigue failure, is the effect of creep fatigue interaction. To explore this aspect of the response a number of specimens were cycled prior to a creep testing. Various combinations of fatigue and creep histories were designed to identify critical underlying assumptions for the mathematical development of a constitutive theory.

In general, the experimental program outlined above was conducted in the stress and strain range of low cycle fatigue and at a constant elevated temperature. Despite the abundance of experimental reports, no report contains the data base outlined above necessary for the analysis and prediction of phenomena like creep-fatigue interaction in the low cycle fatigue domain with fully reversed plasticity.

## II. EXPERIMENTAL PROGRAM

The material used for the study was Refé 95, a high strength nickel-base superalloy developed by General Electric Company and used primarily for compressor and turbine disks in gas turbine engines. A description of the material, processing, heat treatment, microstructure, and composition is given by Menon [1] . The temperature of all tests was 1200°F.

The experiments were conducted at three facilities. The majority of the tests were conducted at the Air Force Materials Laboratory, Metals and Ceramics Division, Wright Patterson AFB, Ohio. These experiments included stress-strain tests on a Instron testing machine at different constant head rates. Also, all tensile creep tests were done of this location on a tensile creep frame using dead weights as the loading device. In all tests a constant gage length specimen was used with an axial extensometer mounted on the shoulders of the test specimen. The extensometer extended from the bottom of a resistance furnace where LVDT gages were used to monitor the axial elongation of the test specimen. The true gage length was estimated using A.S.T.M. standard E139-70.

The compressive creep tests were conducted by Met-Cut Inc., Cincinnati, Ohio. These tests were done also on constant gage length specimens only using an axial extensometer attached directly to the gage section. An induction heater was used and the tests were done on a four-post low cycle fatigue testing machine.

Mar-Test, Cincinnati, Ohio, did one constant strain rate stress-strain test in tension and one in compression; and applied low cycle fatigue damage to five specimens that were shipped to AFML/LLN for subsequent tensile creep tests. They did all work on three-post low cycle fatigue machines

using a diametrical strain gage attached directly to the test section of a constant gage length specimen.

In the tensile tests stress and strain were recorded, and strain and time were recorded in the creep tests. The modulus of elasticity,  $E$ , elastic Poisson ration,  $\nu_e$ , and plastic Poisson ratio,  $\nu_p$ , were used to calculate total true strain,  $\epsilon$ , and the true stress,  $\sigma$ , from the engineering stress,  $\sigma_o$ , and strain,  $\epsilon_o$ . The total strain was written as,

$$\epsilon = \epsilon^I + \frac{\sigma}{E}, \quad (1)$$

the sum of the elastic and inelastic strains. Time derivatives of these quantities were calculated using a generalized central difference technique [2]. The method of data reduction employed was the same as that used by Laflen [3] and Laflen and Stouffer [4,5].

### III. The Stress-Strain Response in Tension and Compression

Several monotonically increasing axial strain tests were conducted in tension over a range of head rates ranging from 0.002 in/min to 0.500 in/min. One constant strain rate test performed at 0.05 in/in/min. The results are shown in Figure 1. The most striking feature of the tests is the large observed variation of elastic modulus, yield stress, and yield strain as recorded in Table 1. Further there does not appear to be any clear ordering of the response with head rate as shown in Table 2. Using this data and low cycle fatigue data it was determined that the nominal elastic modulus at 1200°F is  $25.7 \times 10^6$  PSI.

Suspecting that the elastic parameters could be varying due to the instrumentation, the elastic modulus was adjusted to the nominal value for all tests as shown in Figure 2. The results in Table 2 show that the stress at 1.0% strain is still random with no particular ordering within the observed scatter band. Thus it was concluded from these tests that the material has at most a small strain rate dependence on the range of strain (head) rates examined.

In addition a compressive stress-strain test was run at a strain rate of 0.05 in/in/min. As shown in Figure 3 with the tensile test data run at the same strain rate, there is only a small difference in the tensile and compressive behavior. The curves shown in Figure 3 are used as the nominal tensile and compressive response curves for this study.

Property	Minimum Value	Maximum Value	Nominal Value <sup>(3)</sup>
Elastic Modulus, (PSI x 10 <sup>6</sup> )	17.4	28.8	25.7
Yield Stress in Tension <sup>(1,2)</sup> (KSI)	172.0	184.5	178.0
Yield Stress in Compression <sup>(2)</sup> (KSI)			175.0
Yield Strain in Tension <sup>(1,2)</sup>	0.87%	0.92%	0.90%
Yield Strain in Compression <sup>(2)</sup>			0.88%

(1) Determined with elastic modulus adjusted to  $25.7 \times 10^6$  PSI.

(2) 0.2% offset.

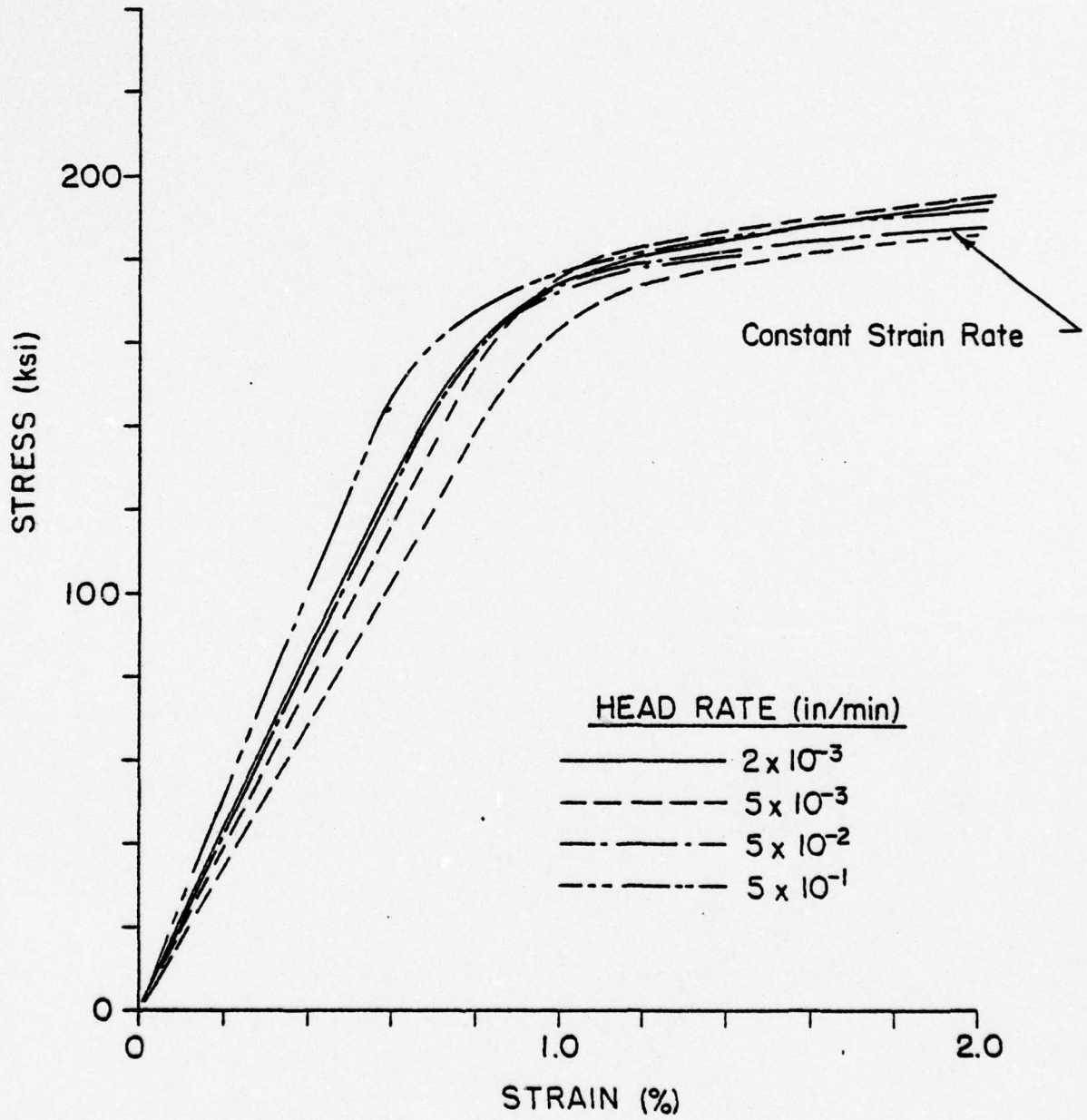
(3) See Figure 3.

Table 1. Variations in Tensile properties of Rene 95 at 1200°F.

Head Rate (in/min)	Mean Stress at 1.0% Strain (KSI)	
	Modulus Not Adjusted	Modulus Adjusted
0.002	185.0	183.0
0.005	182.0	185.7
0.050	177.0	179.0
0.500	186.0	182.5

Table 2. Effect of head rate on the stress at 1.0% total strain.

FIGURE 1 STRESS-STRAIN RESPONSE OF RENE 95 IN TENSION AT DIFFERENT HEAD RATES AT 1200°F



**FIGURE 2**

STRESS-STRAIN RESPONSE OF RENÉ 95 IN TENSION AT DIFFERENT HEAD RATES AT 1200°F WITH THE ELASTIC MODULUS ADJUSTED TO  $25.7 \times 10^6$  PSI.

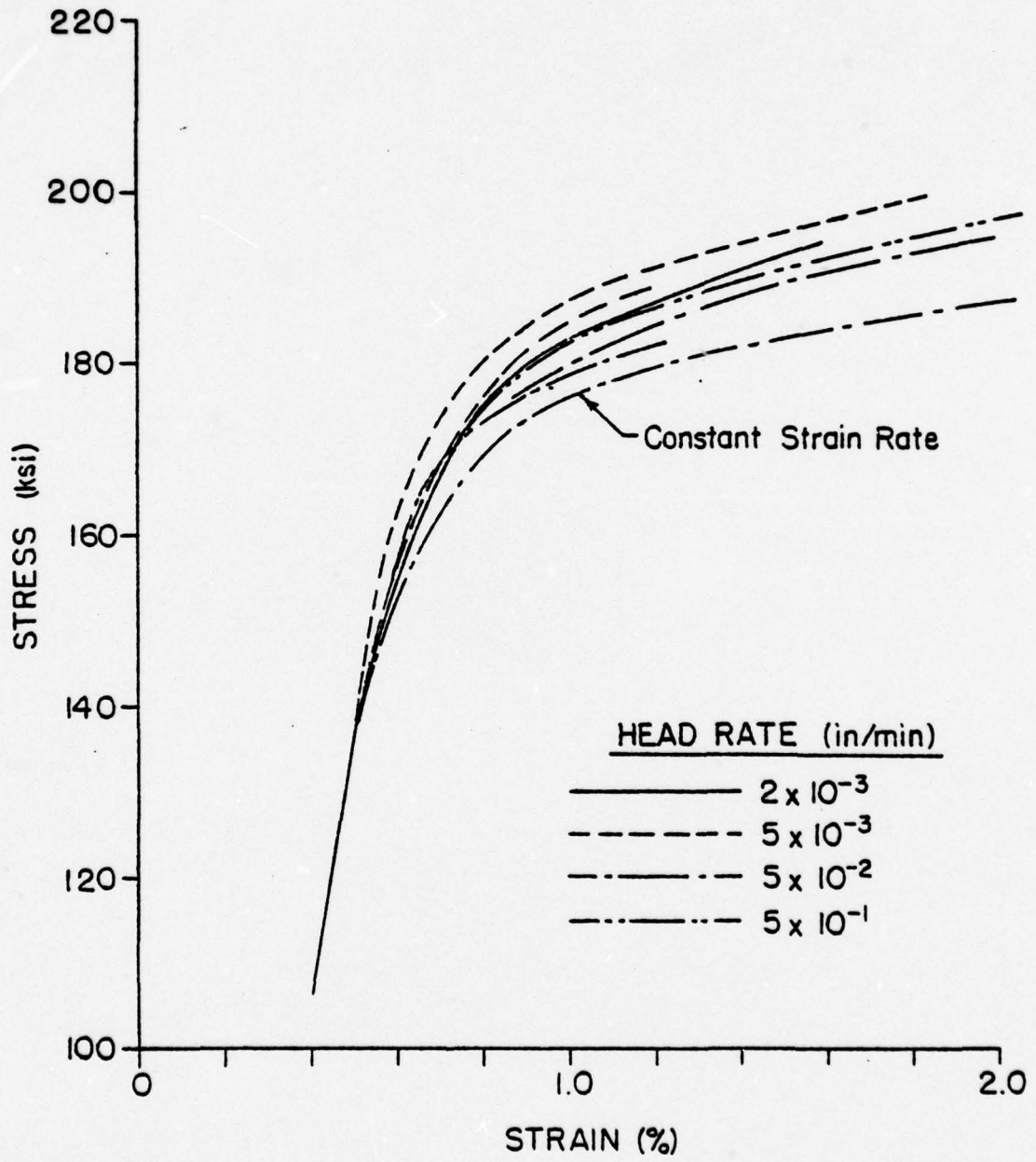
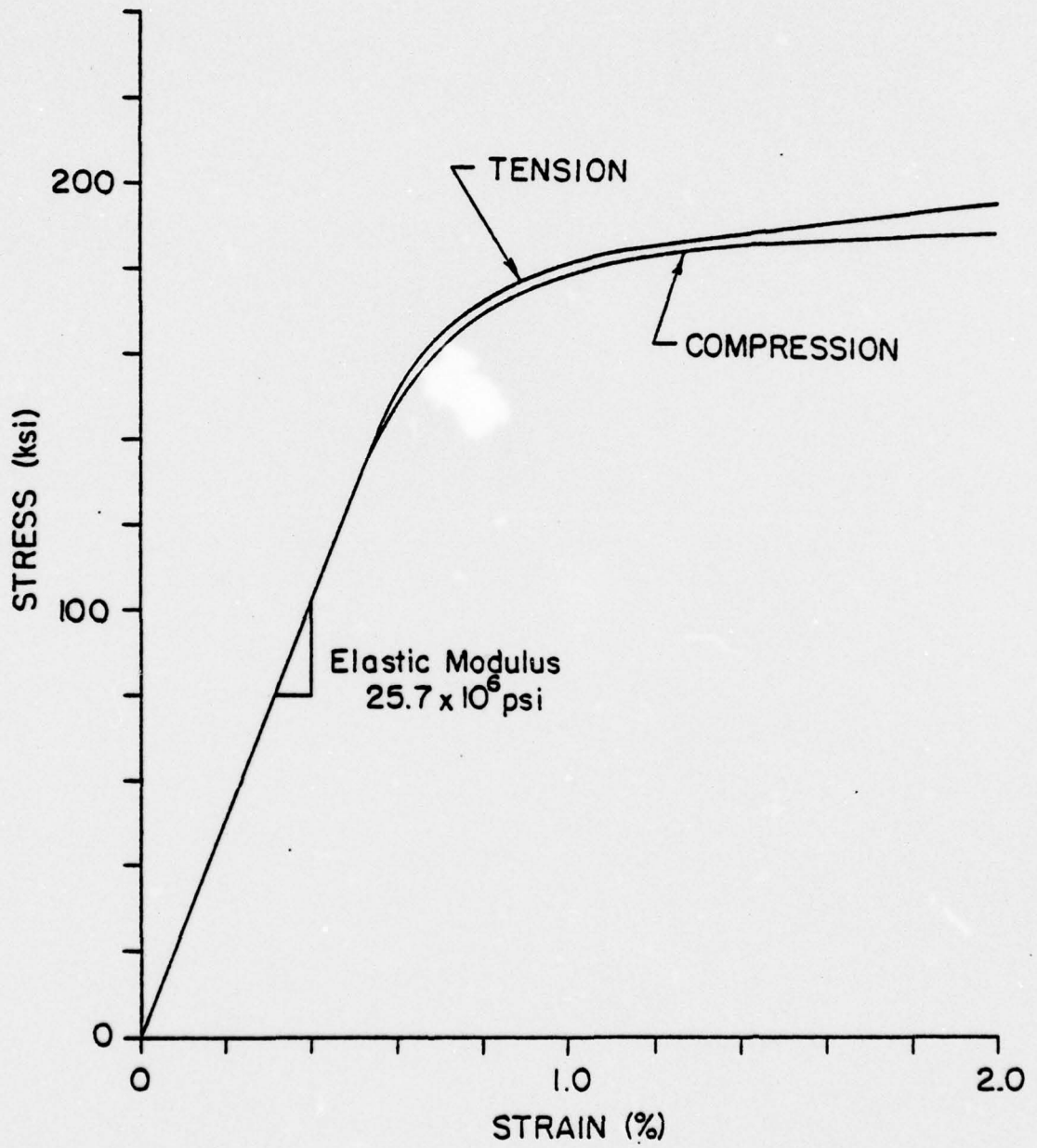


FIGURE 3

COMPARISON OF NOMINAL STRESS-STRAIN RESPONSE OF  
RENÉ 95 IN TENSION TO RESPONSE IN COMPRESSION AT  
1200°F.



#### IV. Creep Tests in Tension and Compression

Standard creep tests were conducted in tension at 184 KSI, 175 KSI, 163 KSI, 150 KSI, and 131 KSI, a range of values from 105% to 75% of the nominal yield stress. In almost all cases the load was applied in less than one minute and duplicate tests were run at 175 KSI, 163 KSI, and 150 KSI. The total response curves to failure are shown in Figures 4 and 5 and a summary of the response characteristics is given in Table 3.

The response of the creep data has been shifted along the strain axis to coincide with the nominal stress-strain response of the material at time  $0^+$ . This is done to provide consistently creep response data.

Similarly, creep tests in compression were run at 184 KSI, 175 KSI, 150 KSI and 131 KSI. The compressive response, except for the 150 KSI test, is shown in Figures 4 and 5 and tabulated in Table 3. The compression tests were terminated at 2 % to 3% strain to avoid buckling failure; however, buckling did occur in two of the four compression tests.

There exists a fairly large variation in the creep-rupture behavior between the duplicate tensile tests at 150 KSI and 175 KSI. The duplicate test, C3, at 163 KSI is quite close as shown, but was prematurely terminated due to a power failure. There is also considerable difference in response between tension and compression at 184 KSI and 175 KSI; however at 131 KSI the response in tension and compression is nearly the same up to 300 hours.

It can be seen in Table 3 that the Tertiary creep phase starts above 1.0% strain in all cases. Since the purpose of this study is to make predictions in the low cycle fatigue range (up to 2% total strain range), a close examination of the primary and secondary creep phase is shown for all tests in Figures 6, 7, and 8. The predominant feature of this response data

is the small amount of primary creep. The slope of the straight line (solid or dashed) through the data points corresponds to the minimum creep rate. In all cases, the duration of the minimum creep rate region is large compared to the primary creep domain. A detailed comparison between tension and compression in the primary and secondary creep domains is given in Section VI.

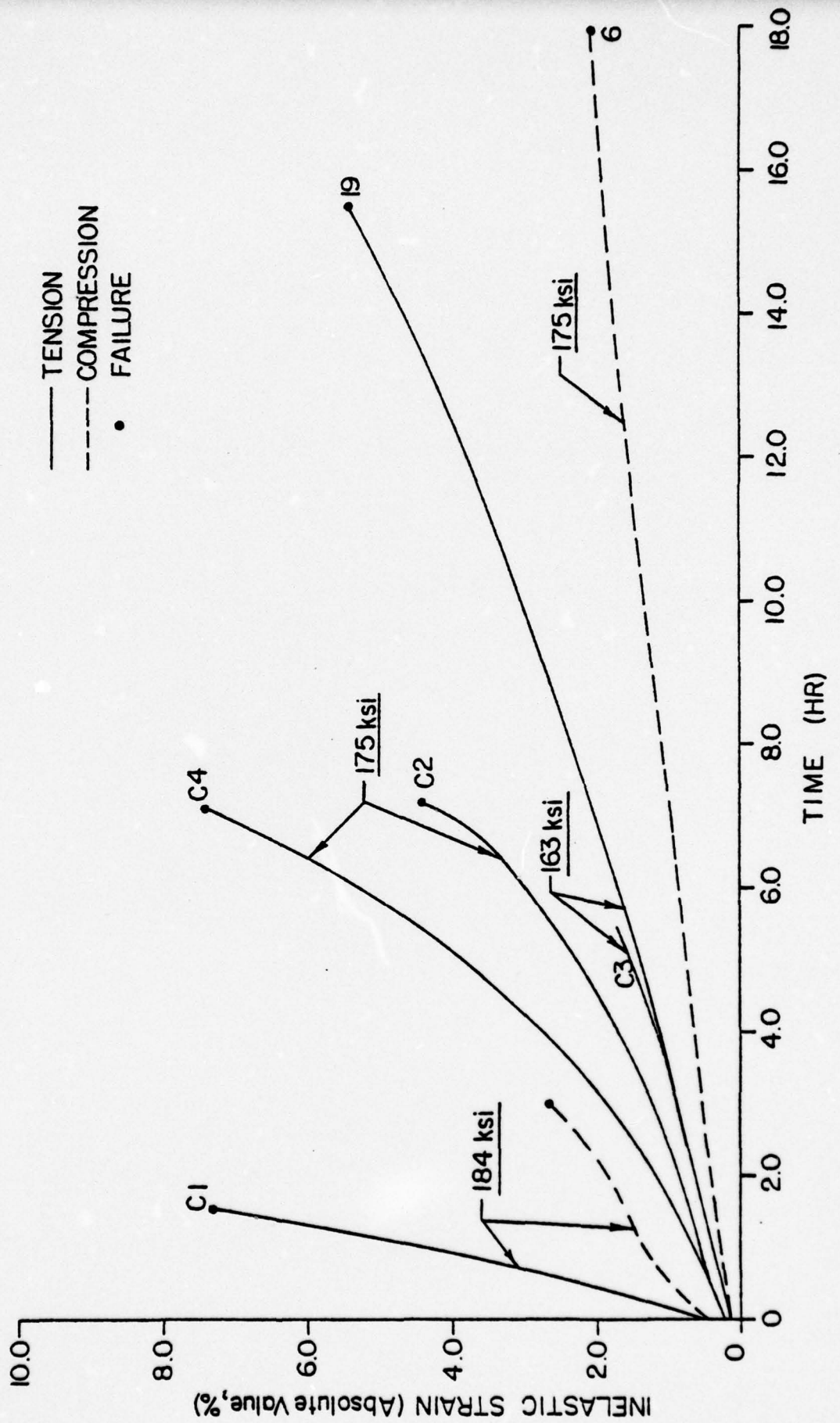
Nominal Stress (KSI)	Specimen Number	Strain At Failure (%)	Time To Failure (HR)	Time To 2.0% Strain (HR)	Initiation of Tertiary Creep (1)	
					Strain (%)	Time (HR)
184T	C1	8.40	1.56	0.25	2.2	0.3
175T	C2	5.15	7.21	3.25	1.2	1.0
	C4	8.49	7.16	2.25	1.3	1.5
163T	19	6.27	15.5	5.0	2.0	5.0
	C3	(Test Stopped)		4.5	1.2	2.0
150T	47	8.30	190.0	75.0	1.5	50.0
	C5	10.8	69.1	16.3	1.8	15.0
131T	20	5.80	504	330	1.1	180.0
184C	1	-3.43 <sup>(2)</sup>	3.0	0.8	2.4	1.5
175C	6	-2.94	18.3	10.0	2.6	15.0
150C	17	-1.37 <sup>(2)</sup>	18.0			
131C	8	-2.07	407.0	394.0	1.01	15.0

(1) Estimate

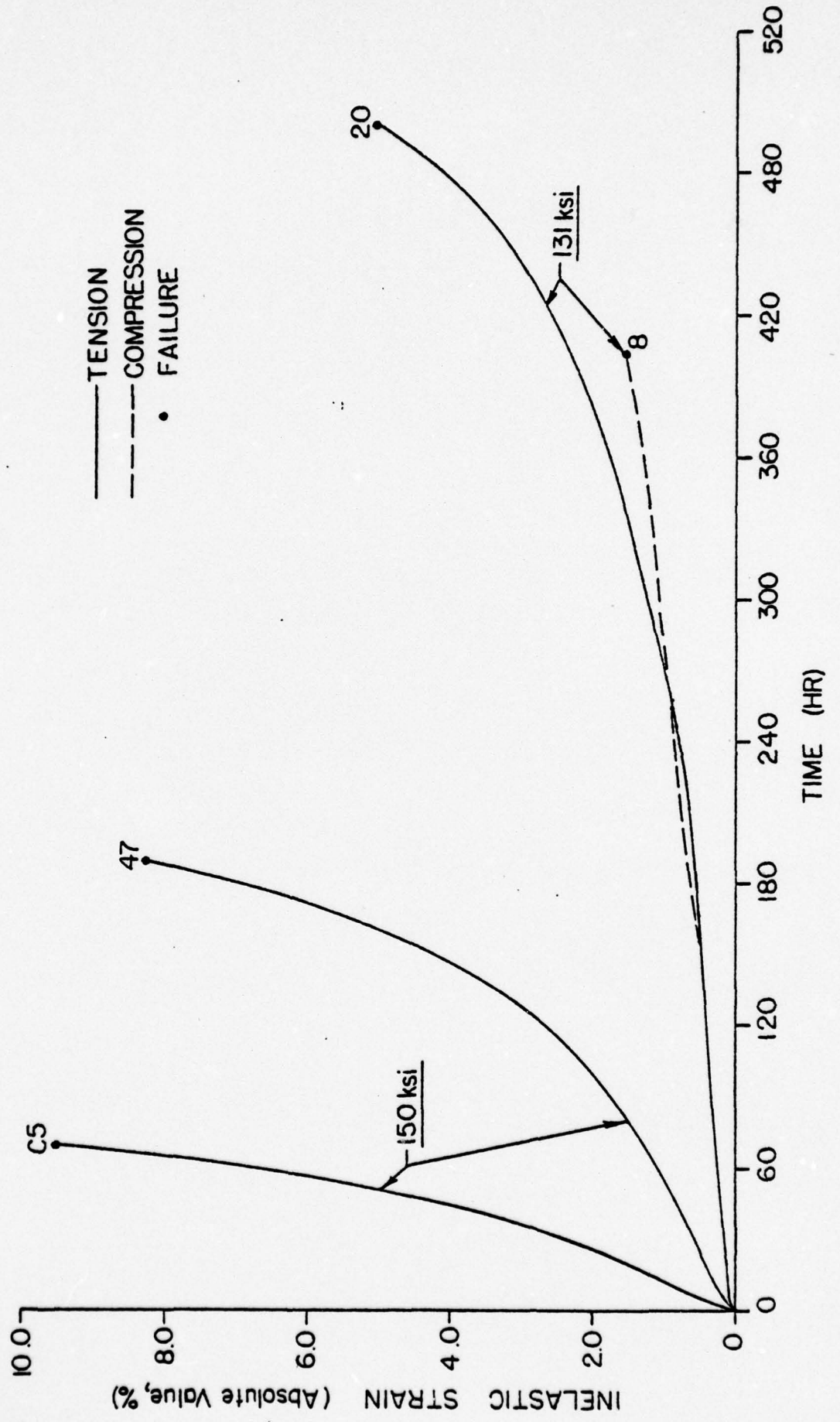
(2) Strain just prior to specimen buckling

Table 3. Summary of creep response of René 95 at 1200°F in tension and compression.

**FIGURE 4** CREEP OF RENÉ 95 AT 1200°F IN TENSION AND COMPRESSION AT 184, 175 and 163 KSI.



**FIGURE 5** CREEP OF RENÉ 95 AT 1200°F IN TENSION AT 150 KSI, AND IN TENSION AND COMPRESSION AT 131 KSI.



**FIGURE 6** PRIMARY AND SECONDARY CREEP OF RENÉ 95 AT 1200°F IN TENSION AT 184 KSI, 175 KSI, 163 KSI AND IN COMPRESSION AT 184 KSI.

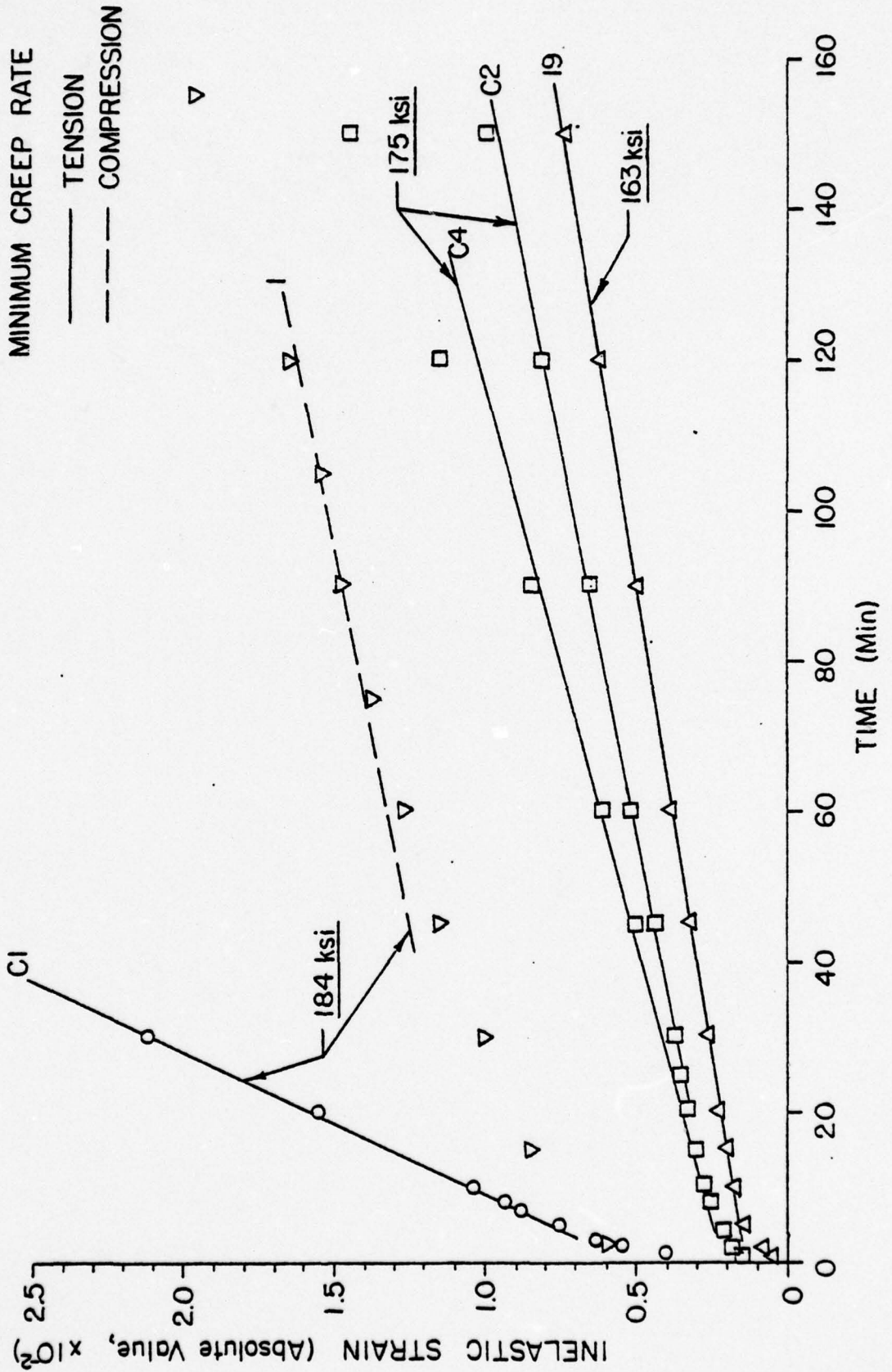


**FIGURE 7** PRIMARY AND SECONDARY CREEP OF RENÉ 95 AT 1200°F IN TENSION AND COMPRESSION AT 150 KSI and 131 KSI.

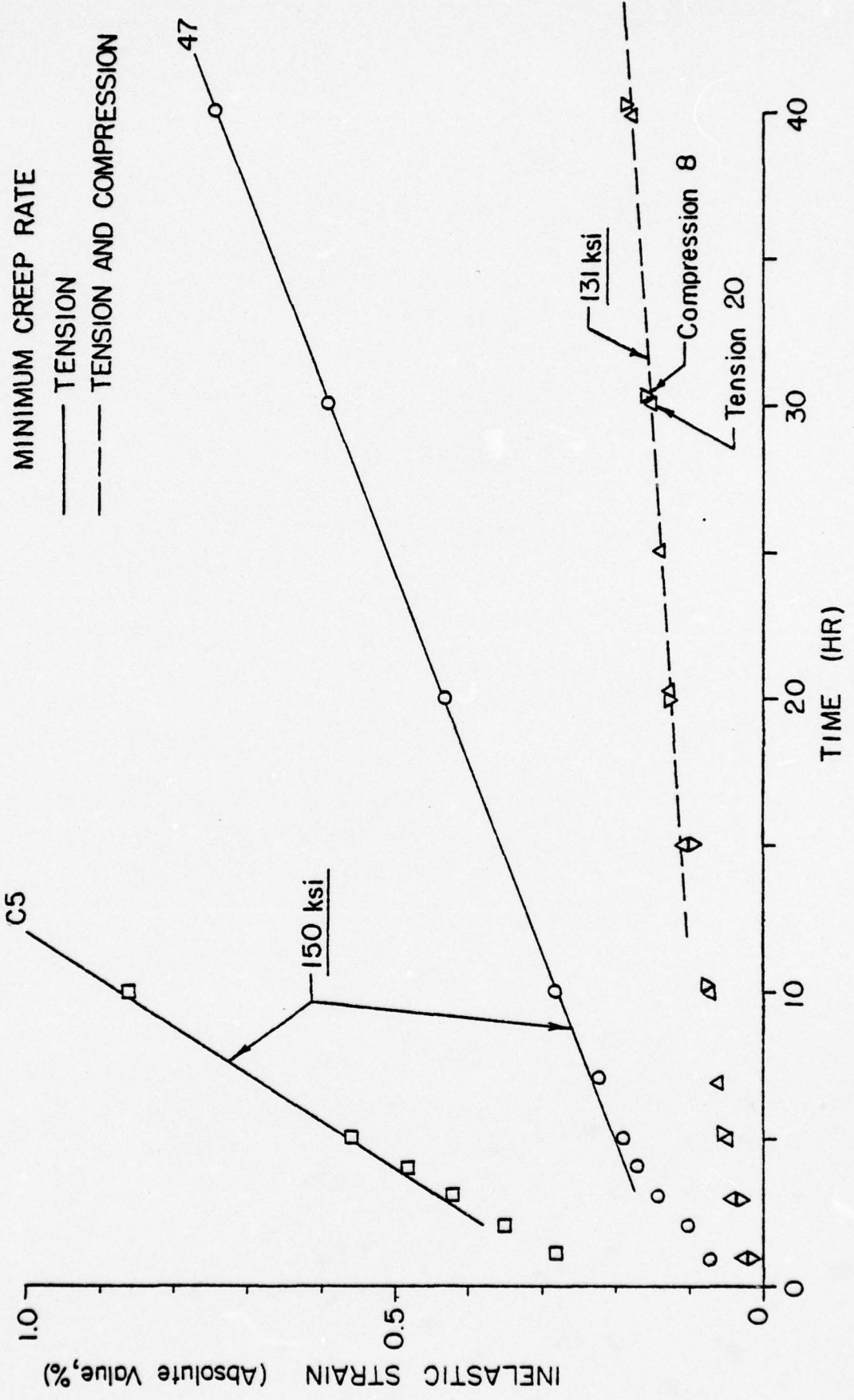
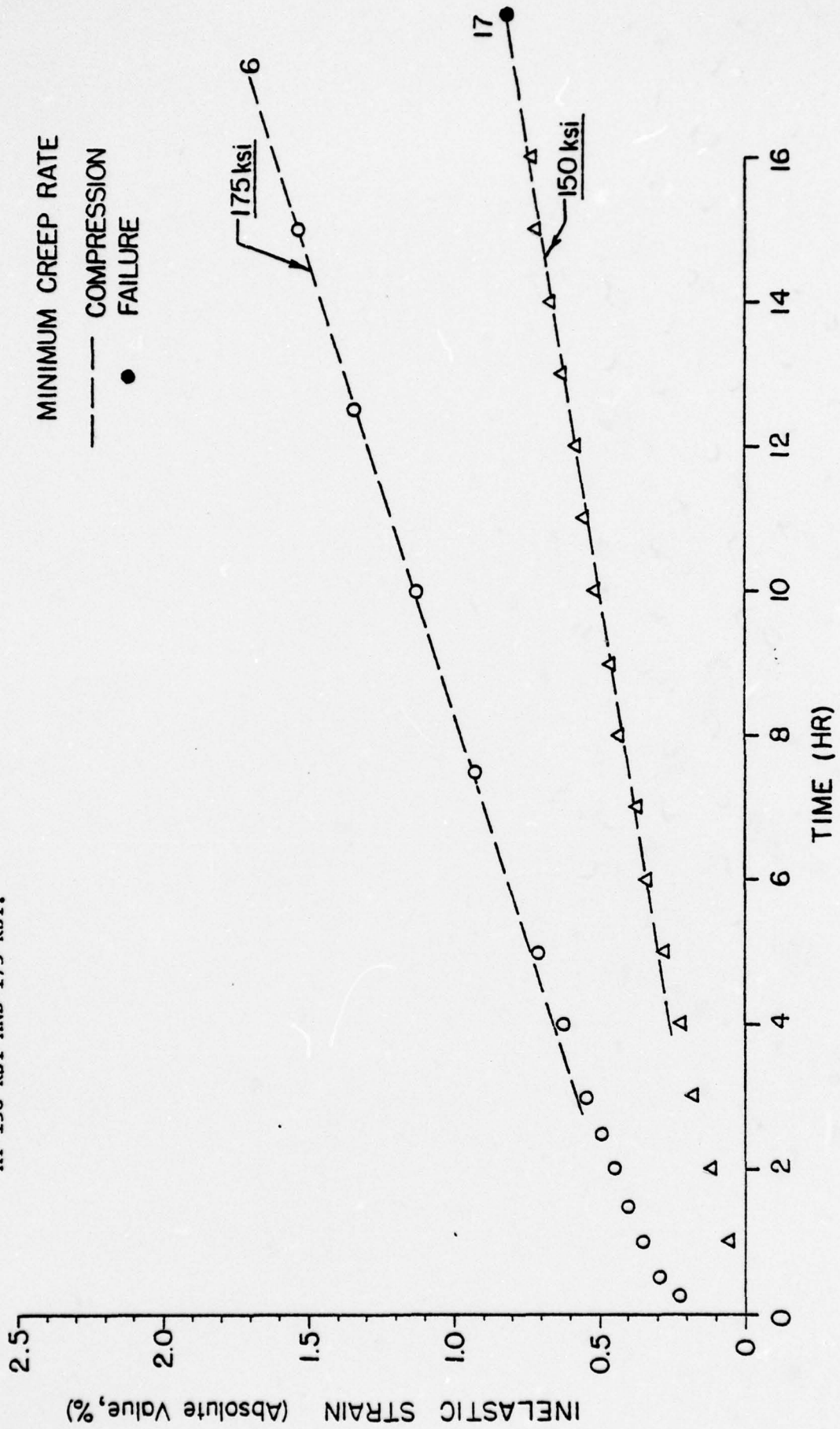


FIGURE 8 PRIMARY AND SECONDARY CREEP OF RENÉ 95 AT 1200°F IN COMPRESSION  
AT 150 KSI AND 175 KSI.



## V. Relationship Between Creep and Stress Relaxation

The creep response curves can be reconstructed as stress-strain curves as a function of time. This is done by plotting the strain obtained from a constant stress creep curve at different times as shown in Figure 9. For example, along the constant stress line at 163 KSI, the strain is plotted at 2, 10, 20, 40, 60, and 90 minutes. All the points at each fixed time are then joined to form a set of isochronis creep curves. <sup>(1)</sup>

An estimate of the stress relaxation can be made by replotting the stress as a function of time at some fixed strain; ie, the intersection of a constant strain line with the family of isochronis curves. The results are shown in Figure 10. for constant strains of 0.6%, 0.7%, and 0.8%. Also plotted on Figure 10 is stress relaxation data observed in the first cycle of fatigue tests for hold times up to 10 minutes. Even though data is for limited times and strains, it does however give reasonably good correlation. Hence, there is reason to expect that the stress relaxation observed in the first few cycles of low cycle fatigue tests with hold times can be predicted relatively well with the creep data. If the effect of fatigue on creep is correctly modeled then the method may be applicable for prediction of stress relaxation in a larger number of cycles.

---

<sup>(1)</sup> The isochronis curves were constructed using the data from specimens C1, C4, 19, and 20.

FIGURE 9

SHORT TIME ISOCHRONIS CREEP CURVES FOR RENÉ 95  
AT 1200°F.

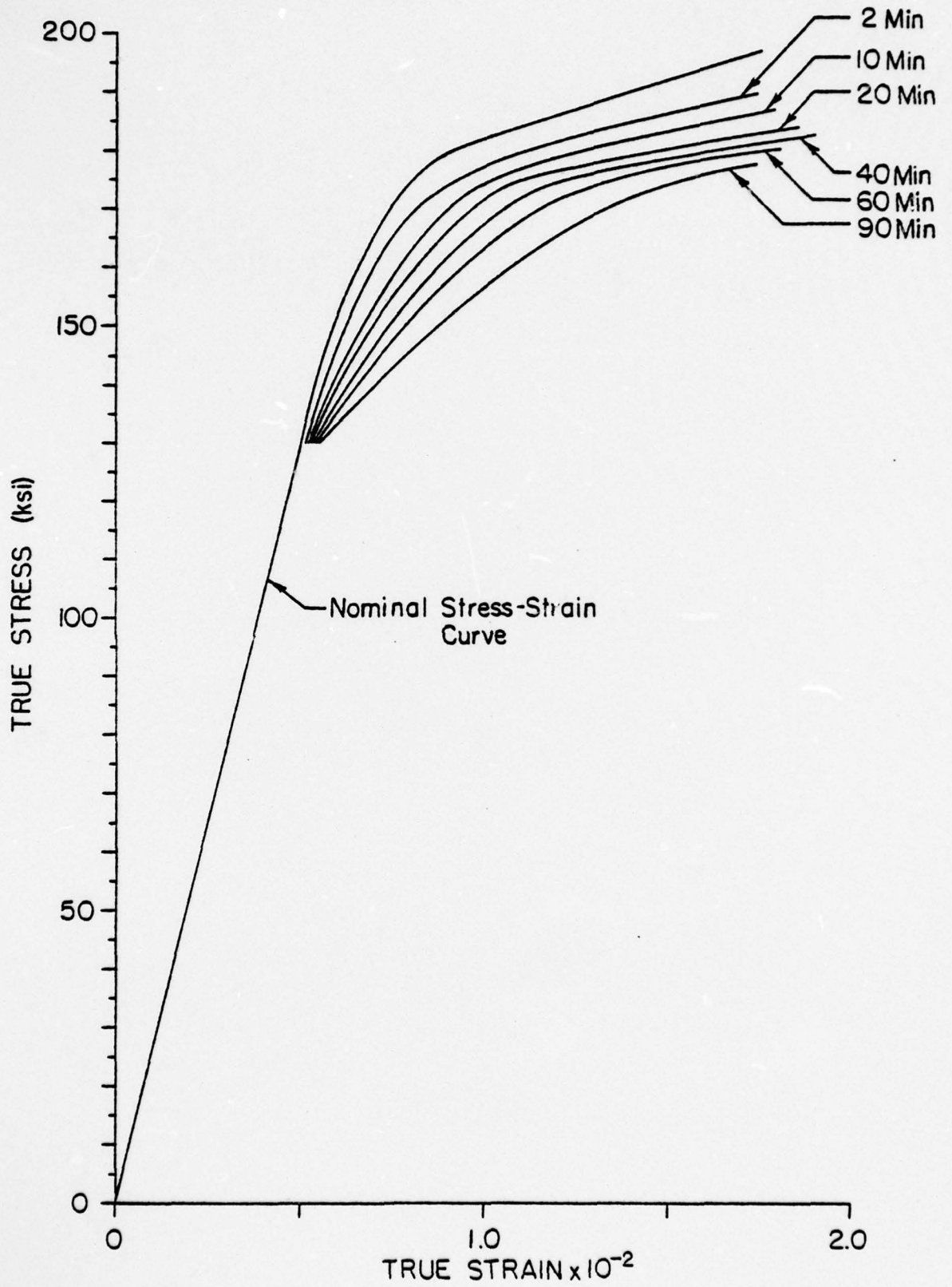
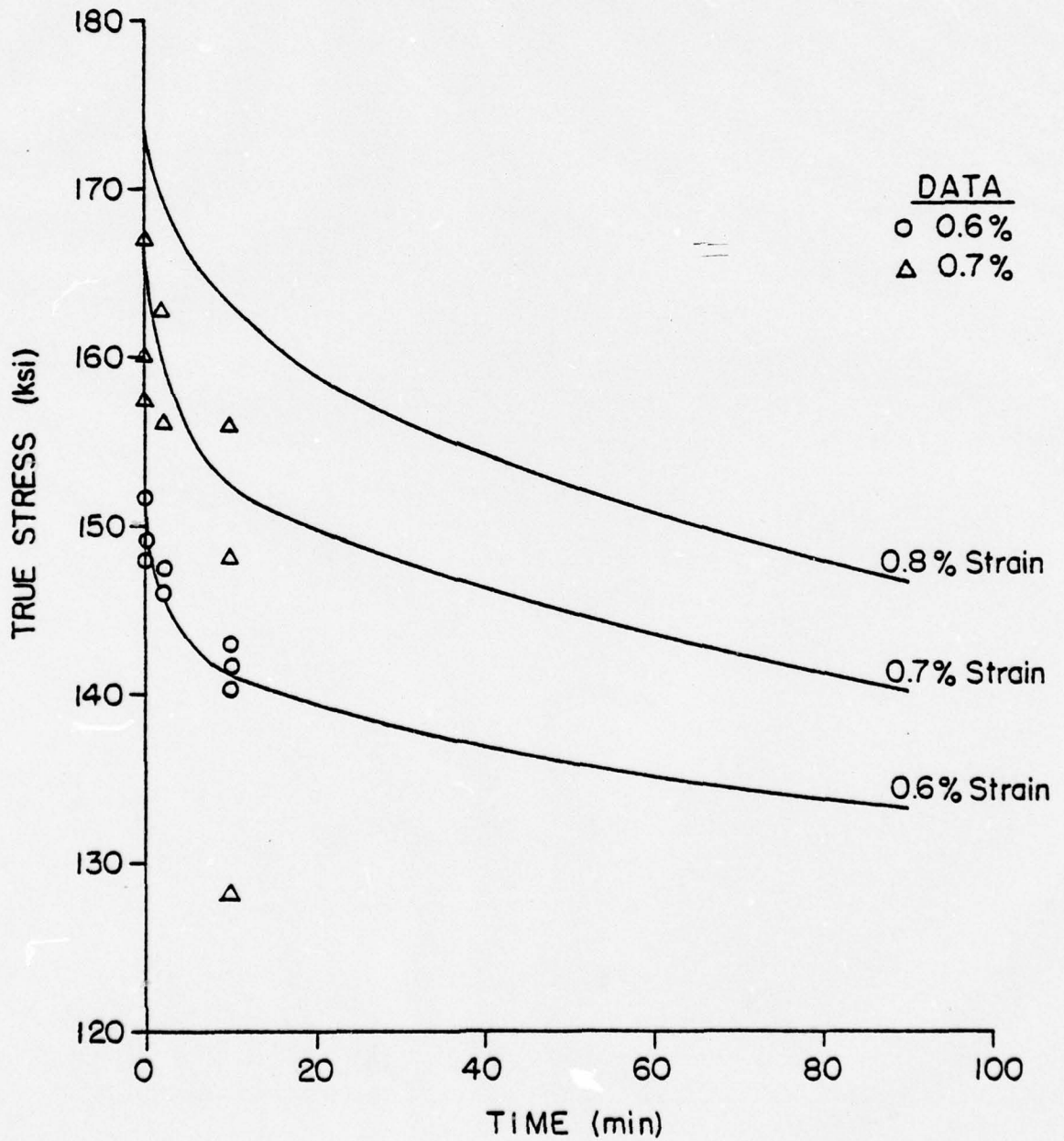


FIGURE 10

COMPARISON OF PREDICTED AND OBSERVED STRESS  
RELAXATION OF RENÉ 95 AT 1200°F.



## VI. A Creep Model

In Section IV the creep response in tension and compression is given for René 95 at 1200°F. This response can be used to determine the functions of a log linear equation [6],

$$\epsilon^I(\sigma, t) = A(\sigma)[1.0 - e^{-\beta(\sigma)t}] + \dot{\epsilon}_m(\sigma)t \quad (2)$$

where  $\epsilon^I$  is the inelastic true strain defined in equation (1). The first term represents primary creep and the second term, linear in time, represents secondary creep. Tertiary creep is not included in the model and has also been deleted from further consideration in the present study. The functions  $A(\sigma)$ ,  $\beta(\sigma)$ , and  $\dot{\epsilon}_m(\sigma)$  of the true stress must be determined from the experimental data. In general, Equation (2) represents the inelastic strain for a constant stress and is not valid for time varying stress since history effects are not included. A constitutive equation for varying stress can be developed using (2) as a material function.

The material functions  $A(\sigma)$ ,  $\beta(\sigma)$ , and  $\dot{\epsilon}_m(\sigma)$  have important physical meanings. Differentiation of equation (2) with respect to time gives

$$\dot{\epsilon}^I(\sigma, t) = A(\sigma)\beta(\sigma)e^{-\beta(\sigma)t} + \dot{\epsilon}_m(\sigma) \quad (3)$$

Setting  $t = 0$  and solving for  $A(\sigma)$  gives

$$A(\sigma) = \frac{\dot{\epsilon}_p(\sigma) - \dot{\epsilon}_m(\sigma)}{\beta(\sigma)} \quad (4)$$

where  $\dot{\epsilon}_p(\sigma) = \dot{\epsilon}^I(0, \sigma)$  is the initial or primary creep rate. Further letting  $t$  become large shows that  $\dot{\epsilon}_m(\sigma)$  is the minimum creep rate of the material.

A procedure for determining the time coefficient has been established in [7] and [3]. Equation (3) can be rewritten as

$$\ln(\dot{\epsilon}^I(\sigma, t) - \dot{\epsilon}_m(\sigma)) = \ln(A(\sigma)\beta(\sigma)) - \beta(\sigma)t \quad (5)$$

thus  $\ln(\dot{\epsilon}^I(\sigma, t) - \dot{\epsilon}_m(\sigma))$  is linear in  $t$ , and the slope of the curve is  $\beta(\sigma)$ . This method to evaluate the tensile data was inadequate since the primary creep response is relatively small and the short time data was poor. Hence, a direct curve fit method was employed and the value of  $A(\sigma)$ ,  $\beta(\sigma)$ , and  $\dot{\epsilon}_m(\sigma)$  for each value of stress was determined, see Table 4. Equation (4) was also used to estimate the primary creep rate  $\dot{\epsilon}_p(\sigma)$ .

The next step is to establish a representation for each of the functions  $A(\sigma)$ ,  $\beta(\sigma)$ , and  $\dot{\epsilon}_m(\sigma)$ . The value of  $A$ ,  $B$ , and  $\dot{\epsilon}_m$  as a function of stress is shown in Figures 11, 12, and 13. The distribution for the minimum strain rate, Figure 11, is slightly different for tension and compression. The strain rate in compression at 150 KSI is not the minimum, but rather the strain rate just before a premature bucking failure. Further, a close examination of the 150 KSI compressive creep data showed that the strain rate had not obtained a minimum. The higher strain rate at 150 KSI in the tensile data is taken as an unexplained bad test.

It is interesting to observe that the data point corresponding to the 184 KSI test in both tension and compression is inconsistent with the rest of the data for all three functions except one, the time coefficient  $\beta$  in tension. This suggests that a different deformation mechanism is activated at the higher stress level. This concept can be further substantiated by carefully examining the stress-strain behavior in tension and compression as given in Table 5. It can be seen that the strain increment corresponding to the stress increment between 175 KSI to 184 KSI is much greater than all other strain increments. Hence there is considerably more plastic flow associated with loading to the 184 KSI stress than with the other stress levels. Since the strain at 184 KSI is an extreme in the range of interest, this response will be excluded from the model.

In general, it can be seen that the tensile and compression responses are different. The most obvious difference is in the time coefficient  $\beta$ . It is constant in compression and increases sharply in tension.

A logarithmic linear fit for the tensile and compressive data has been obtained and the functions are given by:

In Tension

$$A(\sigma) = \exp(-9.16 + 0.0158\sigma) \quad \text{in/in}$$

$$\beta(\sigma) = 2.66 \times 10^{-3} \left(\frac{\sigma}{131}\right)^{22.06} \quad \text{1/min}$$

$$\dot{\epsilon}_m(\sigma) = 4.22 \times 10^{-7} \left(\frac{\sigma}{131}\right)^{17.97} \quad \text{in/in/min}$$

In Compression

$$A(\sigma) = \exp(-12.80 + 0.0422\sigma) \quad \text{in/in}$$

$$\beta = 3.096 \times 10^{-3} \quad \text{l/min}$$

$$\dot{\epsilon}_m(\sigma) = 6.17 \times 10^{-7} \left(\frac{\sigma}{131}\right)^{11.77} \quad \text{in/in/min}$$

where  $\sigma$  is in KSI in all equations. The scatter bands for the data are shown on the figures.

Nominal Stress (KSI)	Specimen Number	Minimum Strain Rate (Min <sup>-1</sup> )	A x 10 <sup>-3</sup> (min <sup>-1</sup> )	β (Min <sup>-1</sup> )	Primary Strain Rate(1) (Min <sup>-1</sup> )
184T	C1	5.30x10 <sup>-4</sup>	4.78	1.209	5.88x10 <sup>-4</sup>
175T	C2	4.98x10 <sup>-5</sup>	2.09	7.38x10 <sup>-1</sup>	2.04x10 <sup>-4</sup>
	C4	6.83x10 <sup>-5</sup>	1.99	6.45x10 <sup>-1</sup>	1.97x10 <sup>-4</sup>
163T	19	3.95x10 <sup>-5</sup>	1.40	3.16x10 <sup>-1</sup>	8.37x10 <sup>-5</sup>
	C3	4.5 x 10 <sup>-5</sup>			
150T	C5	1.11x10 <sup>-5</sup>	2.21	6.88x10 <sup>-2</sup>	1.63x10 <sup>-4</sup>
	47	2.63x10 <sup>-6</sup>	1.42	1.5 x 10 <sup>-2</sup>	2.39x10 <sup>-5</sup>
131T	20	4.46x10 <sup>-7</sup>	0.71	4.35x10 <sup>-3</sup>	3.53x10 <sup>-6</sup>
184C	1	6.30x10 <sup>-5</sup>	9.03	9.35x10 <sup>-2</sup>	9.7x10 <sup>-4</sup>
175C	6	1.33x10 <sup>-5</sup>	3.34	2.63x10 <sup>-3</sup>	2.20x10 <sup>-5</sup>
150C	17	3.47x10 <sup>-6</sup> (2)	1.14	3.38x10 <sup>-3</sup>	9.45x10 <sup>-6</sup>
131C	8	4.73x10 <sup>-7</sup>	0.65	3.28x10 <sup>-3</sup>	2.60x10 <sup>-6</sup>

(1) Calculated from Equation (4).

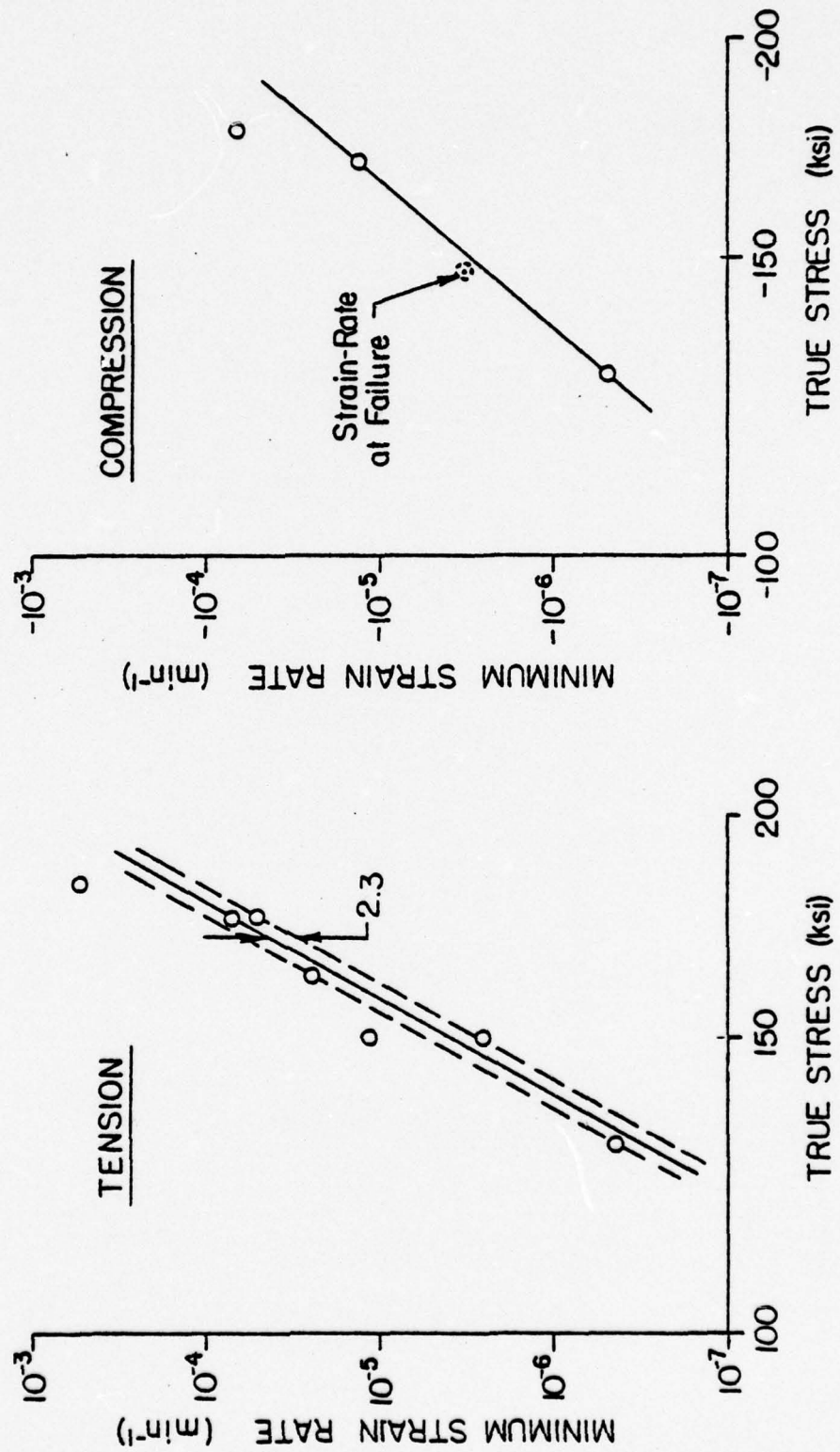
(2) Strain rate just prior to failure

Table 4. Characteristic parameters for the creep response of René 95 at 1200°F

Stress (KSI)	Stress Increment (KSI)	TENSION		COMPRESSION	
		Strain (%)	Strain Increment (%)	Strain (%)	Strain Increment (%)
184		1.12		1.27	
	9		0.30		0.39
175		0.82		0.88	
	12		0.14		0.17
163		0.68		0.71	
	13		0.09		0.10
150		0.59		0.61	
	19		0.08		0.10
131		0.51		0.51	

Table 5. Static response of Rene 95 at 1200°F at the stress levels used for the creep tests.

**FIGURE 11** MINIMUM CREEP RATE OF RENÉ 95 AT 1200°F IN TENSION AND COMPRESSION.



**FIGURE 12** COEFFICIENT A FOR RENE 95 AT 1200°F IN TENSION AND COMPRESSION.

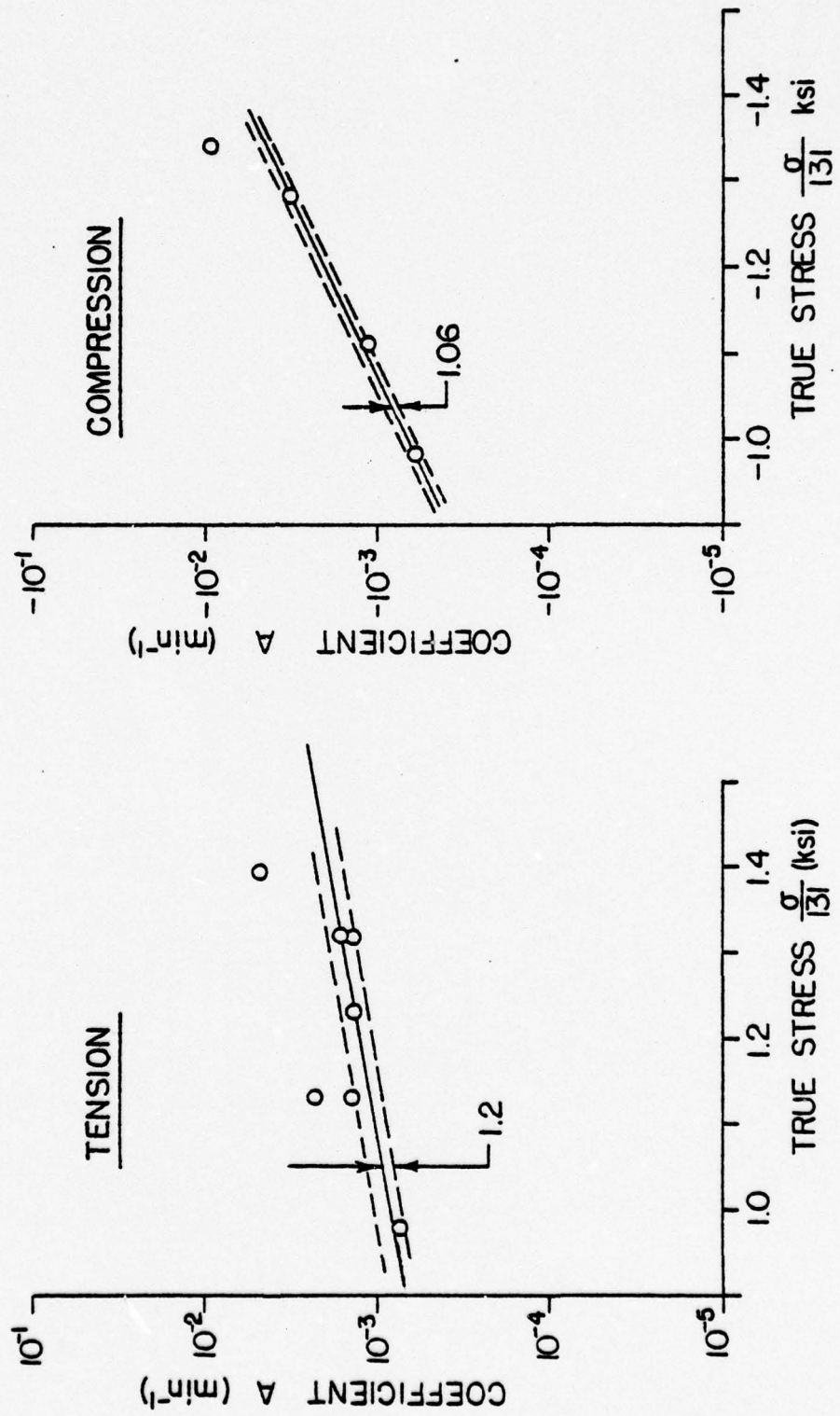
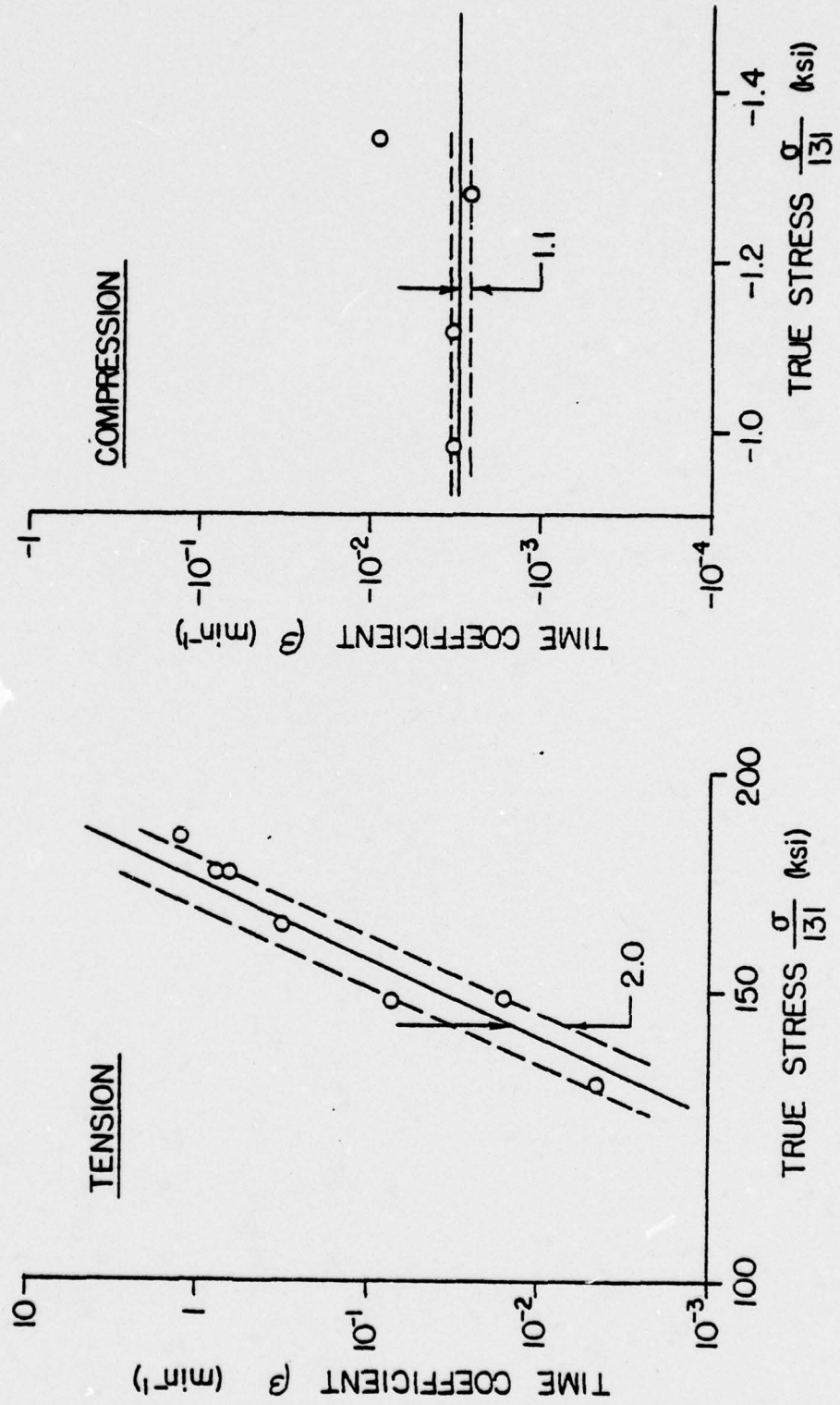


FIGURE 13 TIME COEFFICIENT  $\beta$  FOR RENÉ 95 AT 1200°F IN TENSION AND COMPRESSION.



## VII. Effect of Prior Cyclic Fatigue

Recently in the literature (8,9,10,11) it has been found that cyclic working prior to creep reduces the creep strength of the material for a variety of cyclic softening materials. That is, the time to failure is shorter due to the cyclic softening. Conversely, it might be expected that for a cyclic hardening material, prior working can increase the creep strength of the material. The reverse process; ie, the effect of creep on fatigue, does not appear to have an effect. Ellision and Paterson (13) observed that there was no difference in the low cycle fatigue data between virgin specimens and specimens that had prior creep strain.

Since this type of investigation can reveal many important concepts about both the mechanical response and life of René 95, a preliminary experimental program was established to investigate what aspects of fatigue-creep interactions are present and if they are important.

All the work in the literature has been directed toward showing the effect of various amounts of cyclic damage on creep. Generally it has been found that increasing the fatigue damage increases the effect. This phenomena is assumed to exist and be important for René 95. Thus, rather than investigating the effect of the amount of fatigue damage, it was decided to investigate the effect of stress and strain range on creep for a fixed amount of damage.

Consequently, seven specimens were preworked under a cyclic fatigue program to 21% of the life (as determined from the number of cycles to failure). Five of the specimens were cycled at 1.4% total strain range and two at 1.8% total strain range. The cyclic histories were stopped at two different locations as shown in Figure 14 and Table 6.

One specimen was used for a tensile test to determine if the fatigue history had any effect on the tensile properties. The results of this test are outlined in Table 6. The characteristic response parameters are almost identical to the nominal tensile response.

The remaining specimens were given creep histories at the three stress levels show in Figure 14 in order to answer a number of questions. To raise these questions it is convenient to introduce the following notation for the inelastic strain,  $\epsilon^I$ , as a function of the prework history:

$$\epsilon^I = \epsilon^I(\sigma, \Delta\epsilon_t, \delta, t),$$

where  $\sigma$  is the creep stress,  $\Delta\epsilon_t$  is the strain range,  $t$  is time, and  $\delta$  is defined by

$$\delta = \begin{cases} +1 & \text{if creep strain applied in the same direction as the} \\ & \text{fatigue strain} \\ 0 & \text{if there is no fatigue strain} \\ -1 & \text{if the creep strain is applied in the direction opposite} \\ & \text{to the fatigue strain.} \end{cases}$$

The following questions <sup>were</sup> were investigated with the creep experiments outlined in Table 6.

- a) Since René 95 is a material that hardens at 21% life as shown in the Figure 15, what is the effect of hardening on the creep response?

This can be answered by determining if the ratios

$$\frac{\epsilon^I(175, 1.8, +1, t)}{\epsilon^I(175, 0, 0, t)}$$

and

$$\frac{\epsilon^I(163, 1.4, +1, t)}{\epsilon^I(163, 0, 0, t)},$$

as a function of time, are greater or less than 1.0.

b) Does the strain range of the fatigue cycle effect the creep response?

Mathematically, does

$$\epsilon^I(150, 1.4, +1, t) = \epsilon^I(150, 1.8, +1, t) ?$$

c) If the fatigue cycling does effect the subsequent creep response, is the response independent of stress? That is, does

$$\frac{\epsilon^I(150, 1.4, +1, t)}{\epsilon^I(150, 0, 0, t)} = \frac{\epsilon^I(163, 1.4, +1, t)}{\epsilon^I(163, 0, 0, t)}$$

and

$$\frac{\epsilon^I(150, 1.8, +1, t)}{\epsilon^I(150, 0, 0, t)} = \frac{\epsilon^I(175, 1.4, +1, t)}{\epsilon^I(175, 0, 0, t)}$$

hold, and if so for what time domain?

- d) Is the effect in tension the same as the effect in compression? Since the creep response in tension and compression is different, this can be answered by comparing the following functions of time:

$$\frac{\epsilon^I(163, 1.4, +1, t)}{\epsilon^I(163, 0, 0, t)}, \quad \frac{\epsilon^I(-163, 1.4, +1, t)}{\epsilon^I(-163, 0, 0, t)}$$

- e) What is the effect of reversing the direction of the fatigue cycle with the creep loading? How does

$$\frac{\epsilon^I(163, 1.4, +1, t)}{\epsilon^I(163, 1.4, -1, t)}$$

vary with time?

An outline of the results of the creep tests are given in Table 6. For all tests there was little change in the strain to failure except for specimen 12, that failed 2.01% strain. However, the time to failure was altered in several specimens. At 150 KSI, the time to failure of 69.4 hours was greatly reduced compared to the time of failure of 190 hours for specimen 47, but was nearly the same as specimen c5. Note that the response of specimen c5 did not correlate at all with the other creep tests. At 163 KSI, the time to failure for specimen 16 with the reversed creep load was increased by a

factor of two. At 175 KSI the time to failure was reduced by a factor of two. Similarly, the time of the initiation of the tertiary creep changed in about the same way as the time to failure; but, tertiary creep was initiated at about the same strain level as the tests on virgin specimens.

Since this work is directed toward the primary and secondary creep response, the creep curves for the fatigued specimens in this time domain is shown in Figures 16, 17, 18, and 19. Also shown is the scatter band for nominal response domain that was derived in Section VI to characterize the virgin material. A few general trends can be observed by comparing the response of the preworked creep specimens to the nominal response. First, it appears that the fatigue working enhanced the primary creep response of the material. Second there was relatively little effect on the minimum creep rate. Third, it can be seen from Figure 17 that the effect of reversing the load, as presented in (e) above, is very important.

Another very important feature of Figures 16, 17, and 18 is the extent of the scatter band of the tensile creep data. By comparison, the scatter band for the compressive data is much smaller. Since the material and temperature in both cases is the same, the difference must be the instrumentation and experimental procedures. Further, the accuracy of the measured response for the fatigued creep specimens is the same as the virgin response data making precise comparisons difficult. As a result the calculations proposed in (a) to (e) above are omitted since there is no firm numerical basis for the analysis. Hence, specific details about this part of the study remain unanswered.

Spec No.	PREWORK HISTORY			CREEP HISTORY						
	Strain Range (%)	No. of Cycles	Term Point	Stress (KSI)	Failure Time (HRS) (1)	Failure Strain (%) (1)	Time To 2% Strain (HR) (1)	Minimum Creep Rate (Min <sup>-1</sup> ) (2)	Initiation of Tertiary Creep Strain (%)	Time (HR)
Nominal Response	—	None	—	150	69-190	8.3-10.8	15-50	$1.8-6.0 \times 10^{-6}$	1.5-1.8	15-50
14	1.44	120	A	148	69.4	6.19	27	$5.73 \times 10^{-6}$	1.31	15.0
12	1.80	40	A	150	44.9	2.01	44.9	$3.65 \times 10^{-6}$	1.43	25
Nominal Response	—	None	—	163	15.5	6.27	4.5-5.0	$1.0-39.5 \times 10^{-6}$	1.2-1.5	2.0-5.0
13	1.45	120	A	163	19.7	6.75	4.5	$3.80 \times 10^{-5}$	2.08	5.0
16	1.36	120½	B	163	31.5	5.95	10.0	$1.46 \times 10^{-5}$	2.00	10.0
Nominal Response	—	None	—	175	7.2	5.1-8.5	2.25-3.25	$3.5-11.3 \times 10^{-5}$	1.2-1.3	1.5
11	1.80	40	A	175	3.7	7.78	0.8	$1.88 \times 10^{-4}$	2.47	1.0
Nominal Response	—	None	—	-163	69.5	-3.92	25	$6.02 \times 10^{-6}$	1.55	15.0
9	1.40	120½	B	-163						
10	1.40	120	A							

Tensile Test at  $\dot{\epsilon} = 0.05$  in/in/min.  
0.2% YS = 170 KSI, UTS = 173.4 KSI, E = 25.4y10<sup>6</sup> PSI  
At Failure: Strain = 4.25%, Stress = 143 KSI

(1) Observed Range of Response

(2) Calculated Range of Response.

Table 6. Characteristic parameters showing the effect of fatigue on creep.

FIGURE 14

SCHEMATIC DIAGRAM SHOWING THE DEFORMATION HISTORY APPLIED TO SPECIMENS 9, 11, 12, 13, 14, AND 16.

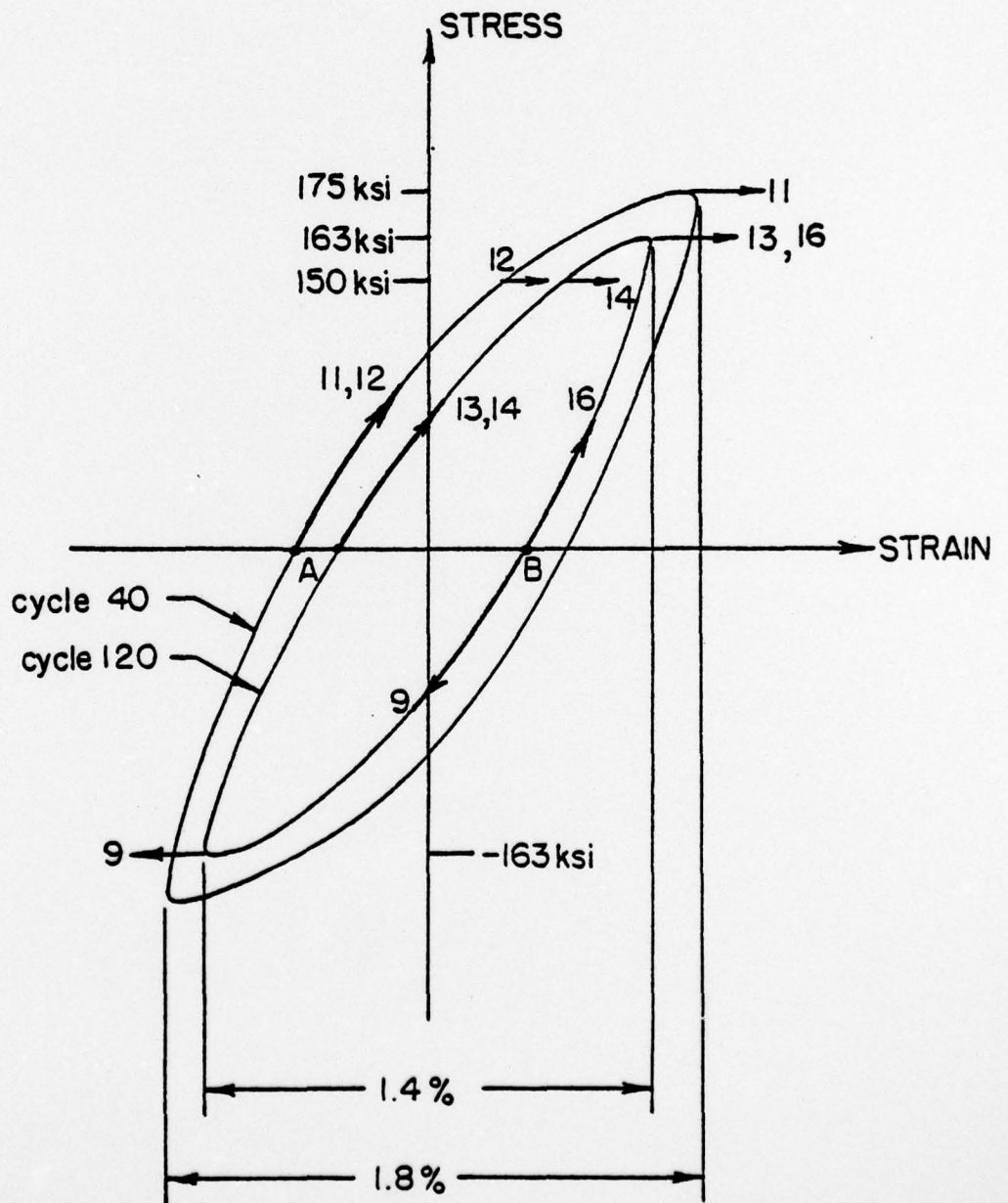


FIGURE 15

(a) THE INITIAL RESPONSE OF A VIRGIN CREEP SPECIMEN.  
(b) INITIAL CREEP RESPONSE OF A SPECIMEN THAT HAS 40 CYCLES OF 1.8% TOTAL REVERSED PLASTIC STRAIN (SPECIMEN 11)

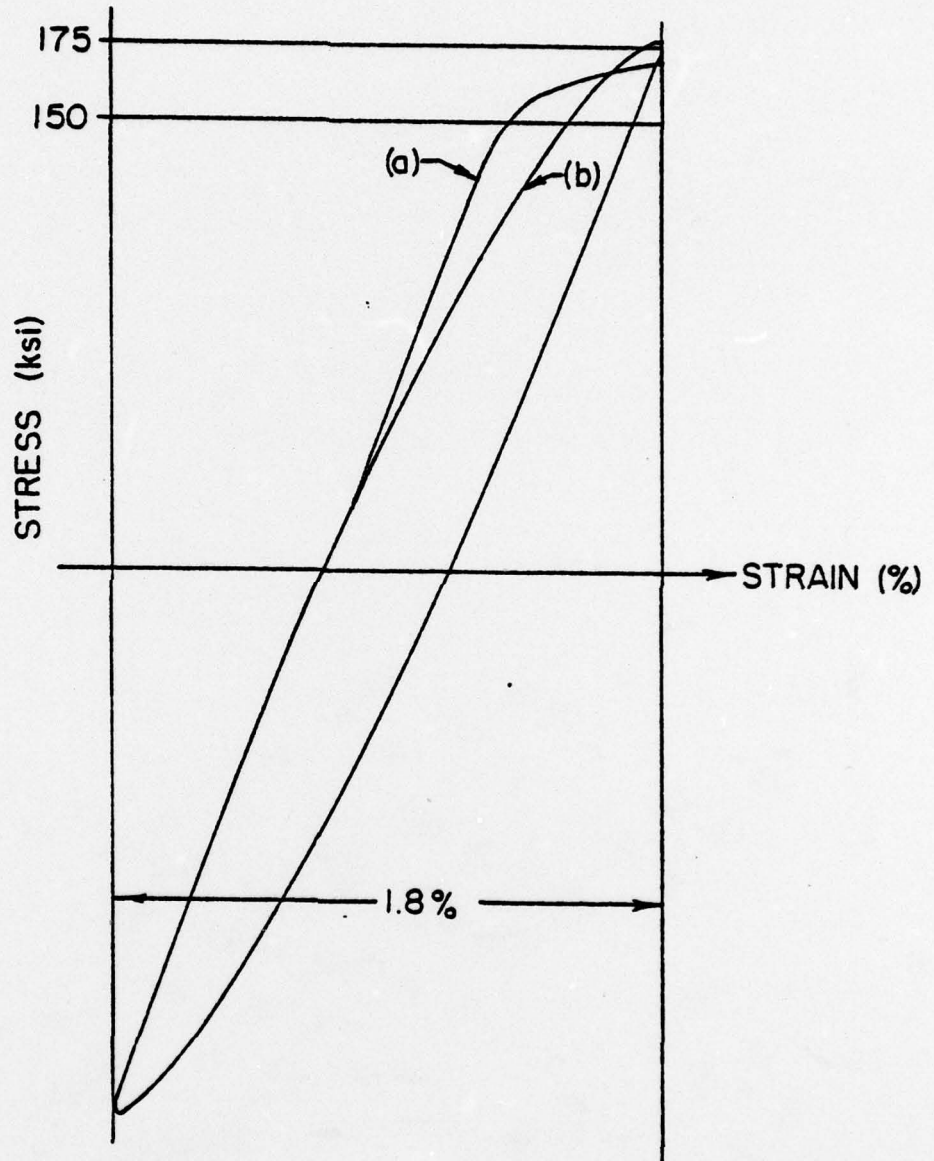


FIGURE 16 EFFECT OF FATIGUE OF THE PRIMARY AND SECONDARY CREEP OF RENÉ 95 AT 1200°F.

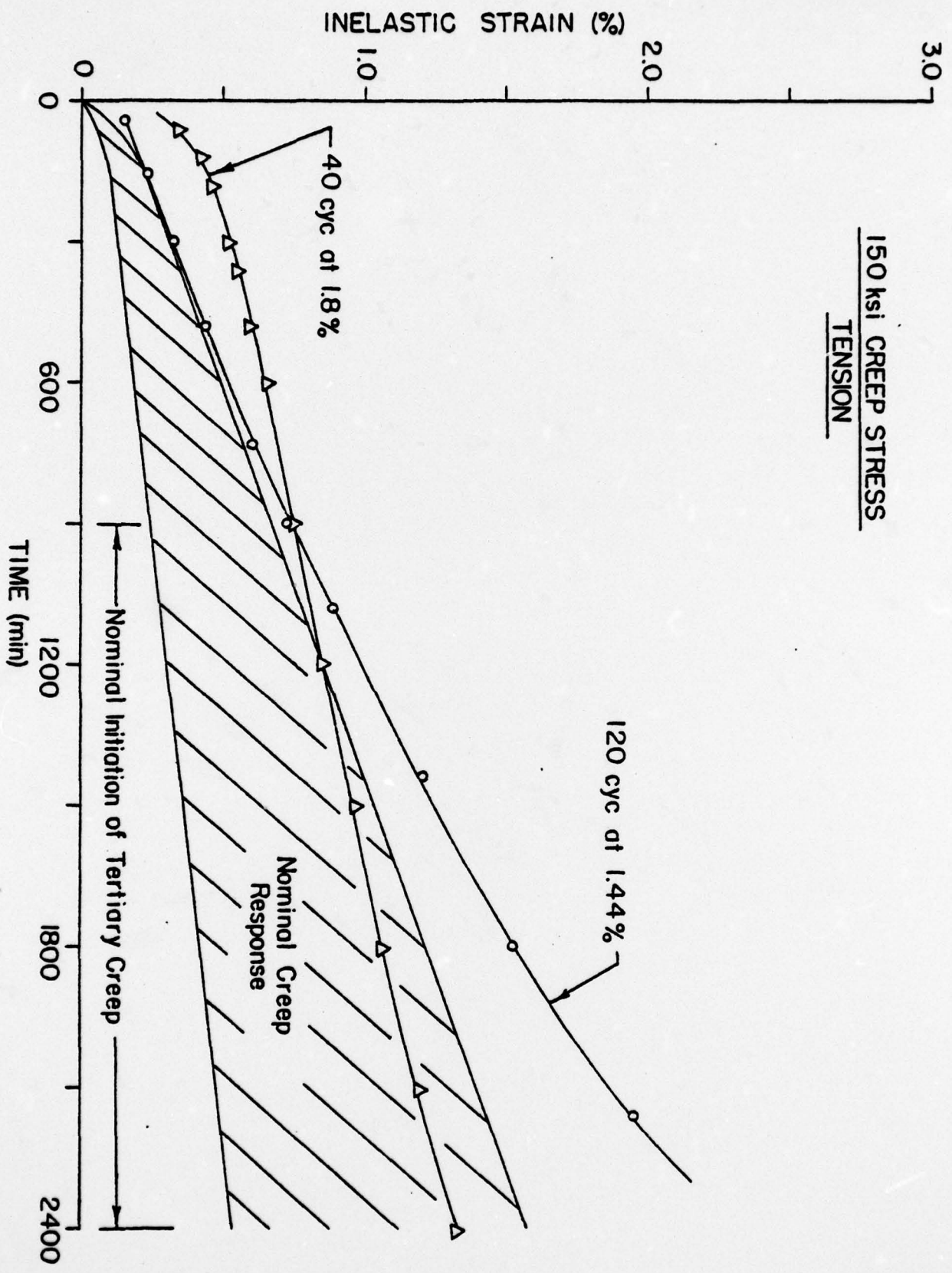


FIGURE 17 EFFECT OF FATIGUE ON THE PRIMARY AND SECONDARY CREEP OF RENE 95 AT 1200°F.

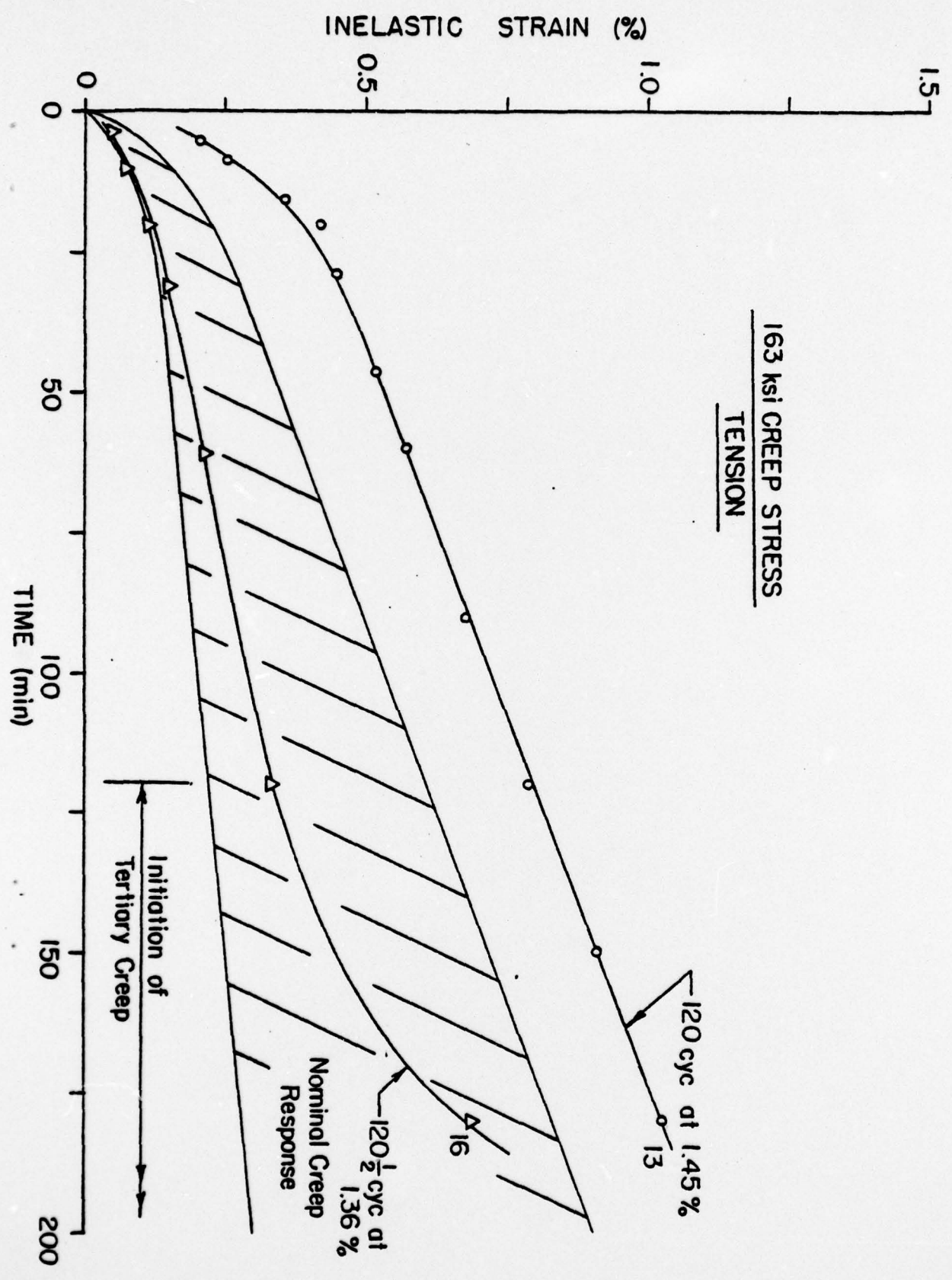


FIGURE 18

EFFECT OF FATIGUE ON THE PRIMARY AND SECONDARY CREEP OF RENÉ 95 AT 1200°F.

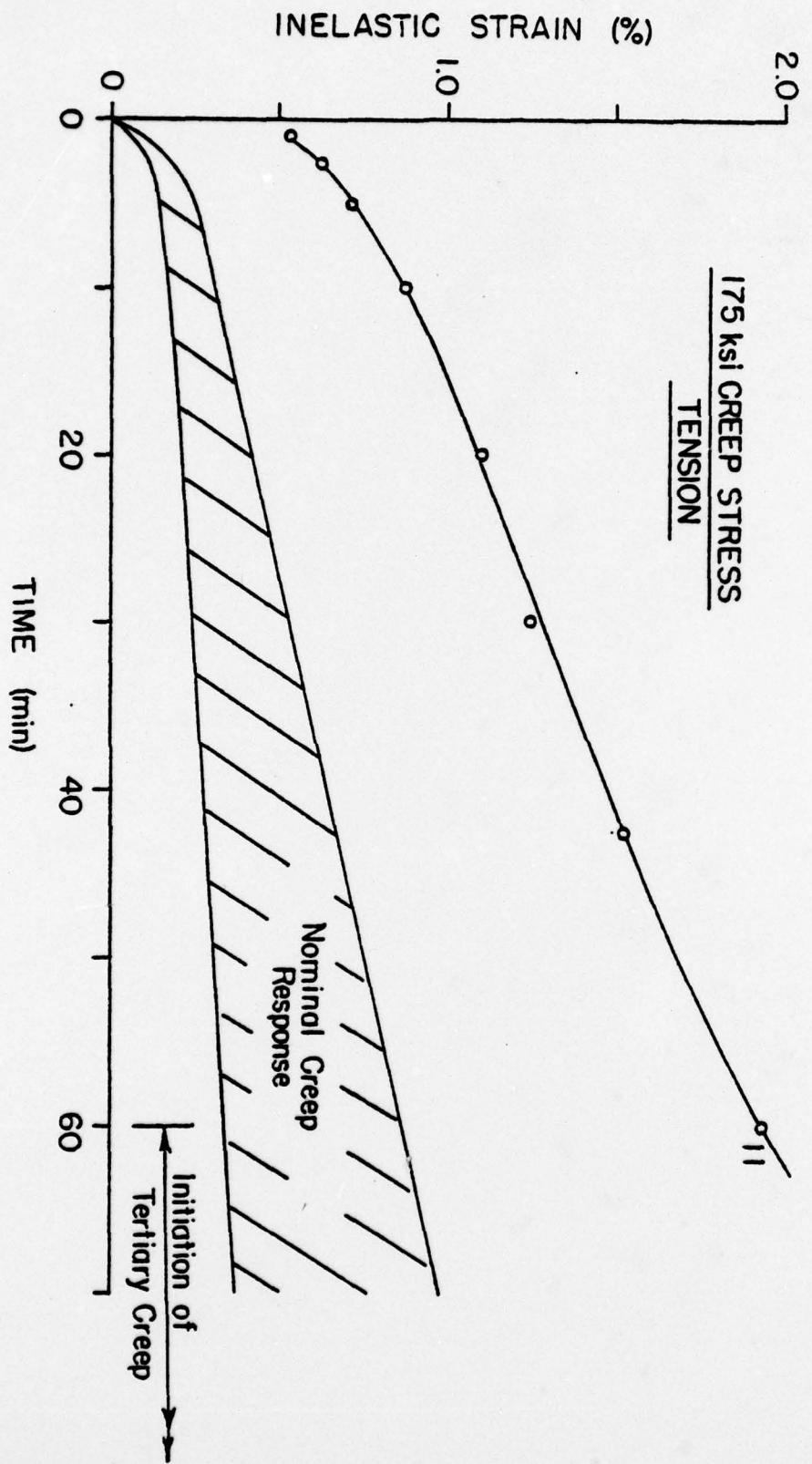
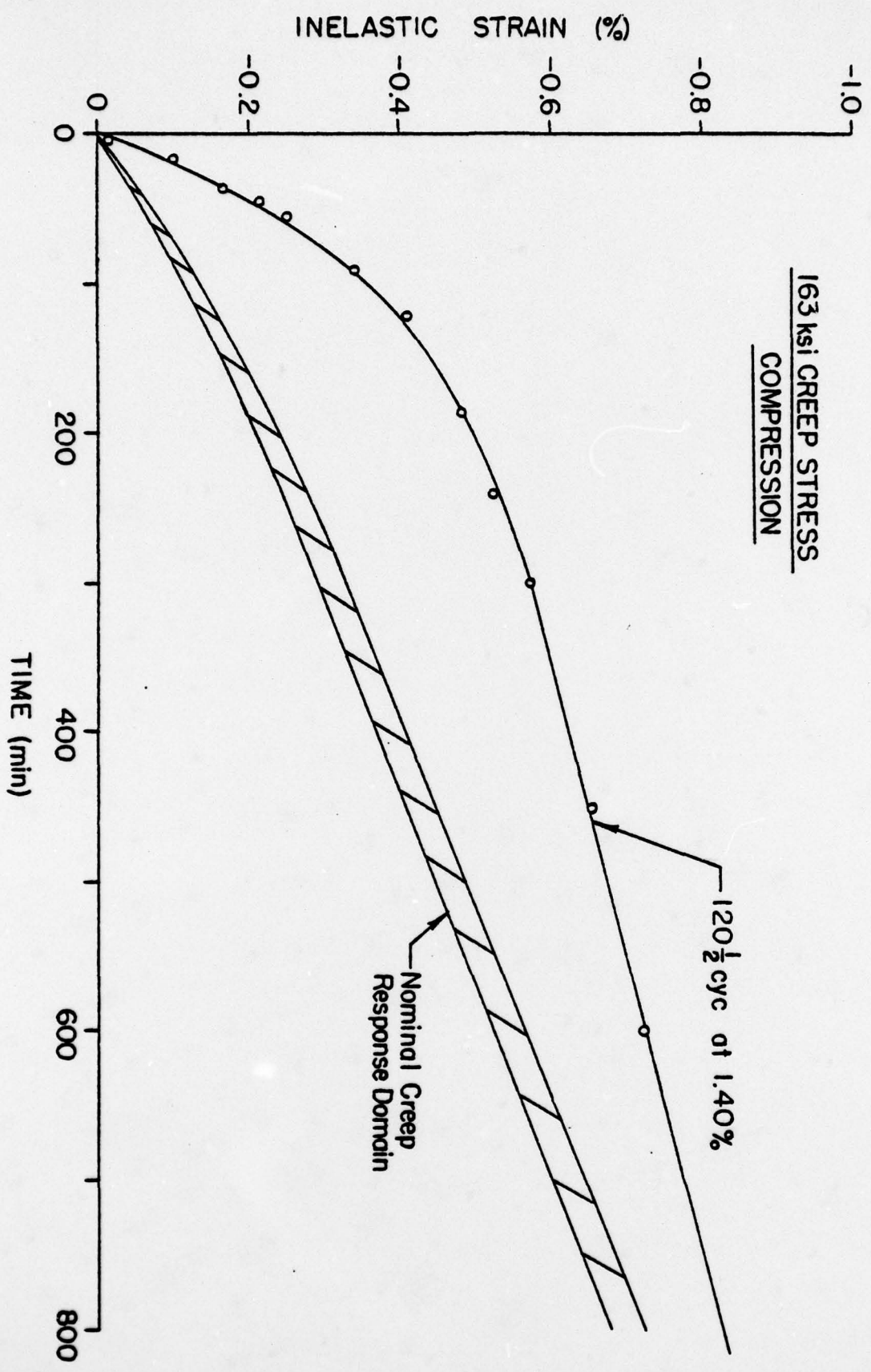


FIGURE 19 EFFECT OF FATIGUE ON THE PRIMARY AND SECONDARY CREEP RESPONSE OF RENÉ 95 AT 1200°F.



### VIII Summary

The major objective of this study is to develop a constitutive representation for René 95 at 1200°F that is valid for variable loading histories.

Recall that the representation developed in Section VI gives the creep strain,  $\epsilon^I(\sigma, t)$ , as a function of stress and time only when the stress is constant.

A general method of analysis has been developed for deriving a constitutive equation for variable stress histories using  $\epsilon^I(\sigma, t)$  as a basic material property<sup>(1)</sup>. The most recent results for high temperature metal creep [5] proposes a constitutive equation of the form

$$\epsilon(t) = \frac{\sigma}{E} + \int_0^t \frac{\partial \epsilon^I(\sigma(\tau), t-\tau)}{\partial (t-\tau)} d\tau + \int_0^t (1-\alpha) \frac{\partial \epsilon^I(\sigma(\tau), \theta)}{\partial \theta} \Big|_{\theta=0} d\tau \quad (6)$$

where  $\epsilon^I$  is the creep response developed above. The material parameter  $\alpha$ ,  $0 \leq \alpha \leq 1$ , controls the relative contribution of viscoelastic and plastic strain. For example, if  $\alpha = 1$ , the equation (5) reduces to the viscoelastic response integral in [12]. Conversely, if  $\alpha = 0$  equation (6) corresponds to a plasticity formulation. The material parameter,  $\alpha$ , depends upon the history of the deformation and must be determined, at least in part, by an experimental program.

Many metals at elevated temperature exhibit a strain rate dependence and a representation for  $\alpha$  has been established using the stress-strain response at different strain rates. The stress-strain evaluation for René 95

---

<sup>(1)</sup>References 4, 5, 12, 13 .

in Section III did not show any clear dependence on time. However, there are certain reservations in presenting this as a firm conclusion. First the stress-strain tests were run at constant head rate which is much different than constant strain rate. Second, even if the effect is small, the results were expected to be ordered. That is, higher strain rates should give higher stress levels. Third, there is clearly a question of the accuracy of the data as evidenced by the unusually large variation in elastic modulus (see Table 1)<sup>(2)</sup>. Fourth, the experiments were over two decades of head rates which is not a very large variation.

An alternative formulation was attempted by investigating the effect of fatigue on creep, which is very important as a fundamental investigation. However, as pointed out in the last section, only general trends were clearly observed. The reliability of the data did not permit the evaluation of the specific questions raised. Since this approach to constitutive equation development is totally unique, a number of fundamental questions as to the important effects must be answered as part of the study. These answers alone would make an important contribution to the literature.

Finally, as seen in equation (6), the inelastic response for a variable stress history is linear in the derivatives of  $\epsilon^I$ . Thus the factor of  $\pm 1.7$  accuracy for tension<sup>(3)</sup> in  $\epsilon^I$  would be directly reflected in the final result. Thus, without even assuming the same level of error in the function  $\alpha$ , the result

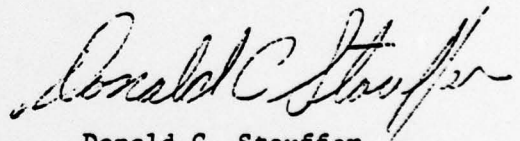
---

(2) The stress-strain data was taken at AFML/LLN using the same techniques as the creep data.

(3)  $\pm 1.06$  for compression.

is totally useless for prediction.

24 February 1978



Donald C. Stouffer  
Associate Professor  
Department of Engineering Science  
University of Cincinnati  
Cincinnati, Ohio 45221

## IX References

- [1] Menon, M.N., "Life Prediction Techniques for Analyzing Creep Fatigue Interaction in Advanced Nickel-Base Superalloys" Air Force Materials Laboratory Technical Report AFML-TR-76-172, Wright Patterson A.F.B. Ohio 45433, Nov. 1976.
- [2] Carnahan, B., Luther H., and Wilkes, J., Applied Numerical Methods, John Wiley and Sons, New York, 1969.
- [3] Laflen, J.H., "A Constitutive Theory for Metal Creep", Ph.D. dissertation, University of Cincinnati, Cincinnati, Ohio, 1976.
- [4] Laflen, J.H., and Stouffer D.C., "An Analysis of High Temperature Metal Creep, Part I. Experimental Definition of a Alloy", Department of Engineering Science Report, ES 77-114, University of Cincinnati, Cincinnati, Ohio 45221, (1977).
- [5] Laflen, J.H. and Stouffer, D.C., "An Analysis of High Temperature Metal Creep. Part II. A Constitutive Formulation and Verification" Department of Engineering Science Report ES 77-115, University of Cincinnati, Cincinnati, Ohio 45221, (1977).
- [6] Pao, Y.H. and Marin, J., "An Analytical Theory of the Creep Deformation of Materials". Journal of Applied Mechanics, 20.2, pp. 245-252, (1953).
- [7] Conway, J.B., Numerical Methods for Creep and Rupture Analyses, Gordon-Breach Science Publishers, (1967).
- [8] Plumbridge, W.J. and Miller, K.J., "Influence of Prior Fatigue on the Creep on 'Non-Heat-Treated' alloy Steel", Metal Technology, pp. 249-252, 1975.
- [9] Ellison, E.G. and Paterson, A.J.F., "Creep Fatigue Interactions in a I Cr. Mo. V Steel", Proceedings Instn. Mech. Engrs., V190, pp. 321-332, 1976.
- [10] Ellison, E.G. and Paterson, A.J.F., "Behavior of a I Cr. Mo. V Steel Subject to Combinations of Fatigue and Creep Under Strain Control", Proc. Instn. Mech. Engrs. V190, pp. 333-340, 1976.
- [11] Sidey, D., "Creep-Fatigue Interactions in a Low-Alloy Steel", Fracture 1977, Vol. 2, Proc. 4th Intern. Conf. on Fracture, Waterloo, Canada, 1977.
- [12] Stouffer D.C., "A Single Integral Constitutive Law for Weak Non-Linear Viscoelastic Solids", Int. J. Non-Linear Mechanics, 7, pp. 465-472, (1972).
- [13] Stouffer, D.C., "Environmental Effects on Stress Analysis of Viscoelastic Materials" AIAA Journal, 13.11, pp. 1508-1513, (1975).

REPORT DOCUMENTATION PAGE		READ INSTRUCTIONS BEFORE COMPLETING FORM
1. REPORT NUMBER AFOSR-TR- 78-0905 ✓	2. GOVT ACCESSION NO.	3. RECIPIENT'S CATALOG NUMBER
4. TITLE (and Subtitle) AN EVALUATION OF THE MONOTONIC RESPONSE OF RENE 95 AT 1200 DEGREE F		5. TYPE OF REPORT & PERIOD COVERED FINAL 15 Dec 76 - 14 Dec 77
		6. PERFORMING ORG. REPORT NUMBER
7. AUTHOR(s) DONALD C STOUFFER		8. CONTRACT OR GRANT NUMBER(s) AFOSR 77-3101 <i>new</i>
9. PERFORMING ORGANIZATION NAME AND ADDRESS UNIVERSITY OF CINCINNATI DEPARTMENT OF ENGINEERING SCIENCE ✓ CINCINNATI, OHIO 45221		10. PROGRAM ELEMENT, PROJECT, TASK AREA & WORK UNIT NUMBERS 2307D9 61102F
11. CONTROLLING OFFICE NAME AND ADDRESS AIR FORCE OFFICE OF SCIENTIFIC RESEARCH/NA BLDG 410 BOLLING AIR FORCE BASE, D C 20332		12. REPORT DATE Feb 78
14. MONITORING AGENCY NAME & ADDRESS (if different from Controlling Office)		13. NUMBER OF PAGES 51
		15. SECURITY CLASS. (of this report) UNCLASSIFIED
		15a. DECLASSIFICATION/DOWNGRADING SCHEDULE
16. DISTRIBUTION STATEMENT (of this Report)  Approved for public release; distribution unlimited.		
17. DISTRIBUTION STATEMENT (of the abstract entered in Block 20, if different from Report)		
18. SUPPLEMENTARY NOTES		
19. KEY WORDS (Continue on reverse side if necessary and identify by block number) RENE 95 CREEP STRESS RELAZATION STRESS-STRAIN RESPONSE CREEP FATIGUE INTERACTION		
20. ABSTRACT (Continue on reverse side if necessary and identify by block number) The general objective of this study is to develop a constitutive equation for rene 95 at 1200°F. The analysis is limited to deformations in the low cyclic fatigue range of the material. A number of stress-strain and creep experiments were run at temperature to characterize the mechanical response properties of the material. A model was developed for the primary and secondary creep of the material. An investigation of the effect of fatigue on creep was carried out to determine the importance of the creep stress level, fatigue strain range, and the fatigue-creep sequence. In general it was found that the primary creep was greatly enhanced with relatively little effect on the minimum creep rate.		